Investigating the cooling effect of a green roof in Melbourne

Jamei, Elmira, Thirunavukkarasu, G, Chau, Hing-Wah, Seyedmahmoudian, M, Stojcevski, A and Mekhilef, S (2023) Investigating the cooling effect of a green roof in Melbourne. Building and Environment, 246. ISSN 0360-1323

Building and Environment 246 (2023) 110965

Contents lists available at ScienceDirect

Building and Environment

journal homepage: www.elsevier.com/locate/buildenv

Investigating the cooling effect of a green roof in Melbourne

E. Jamei [a,b,*], G. Thirunavukkarasu [c], H.W. Chau [a,b], M. Seyedmahmoudian [c], A. Stojcevski [c], Saad Mekhilef [c]

[a] Institute of Sustainable Industries and Liveable Cities, Victoria University, Australia
[b] College of Sport, Health and Engineering, Victoria University, Australia
[c] School of Science, Computing, and Engineering Technologies, Swinburne University of Technology, Australia

ARTICLE INFO

Keywords:
Green roof
Urban heat island
Pedestrian thermal comfort
ENVI-met

ABSTRACT

'Green Our Rooftop' aims to transform the rooftop of Treasury Place, a state government building in the inner city of Melbourne, into an intensive green roof under the notion of 'Garden of Victorian Landscapes'. The concept behind the innovative green roof design is to break down perceived barriers to green roof retrofitting, limit the global temperature rise and help cool the city by advocating modifications in urban infrastructure (e.g. greening projects). This study quantified the cooling effect of the complex green rooftop of Treasury Place (which is characterised by a diverse range of plant types and topographies) by using ENVI-met to assess the air temperature and outdoor thermal comfort at rooftop and pedestrian levels. After verification through field measurements, the study also investigated how the adjustments in the green roof's design settings (e.g. leaf area index [LAI], plant height, soil moisture and additional green coverage) can further improve the green roof's thermal performance. The findings from our study indicate that the implemented green roof configuration effectively lowered the air temperatures at the roof level by 1.5 °C, simultaneously enhancing thermal comfort by 2.38 °C during hot summer days. This optimum performance was achieved when soil moisture levels were set at 0.6, plant height at 0.6, and LAI at 2.5. Our statistical analysis indicates that all these scenarios exhibited equivalent cooling benefits. Thus, a holistic approach optimizing LAI, plant height, soil moisture, and tree coverage combined is essential to maximise cooling impact when integrating green roofs into future developments in inner city areas.

1. Introduction

Urban land areas in the world are expected to increase by around 1.5 million km^2 by 2030, which is three times larger than the urban land area in 2000 [1]. Therefore, revisiting the design and planning guidelines for new urban developments and creating balance between natural and built environments are urgently needed. Climate change effects are more tangible in urban areas than in rural ones due to the high level of human-induced heat, and this is the main reason urban centres are a few degrees warmer than their surrounding rural areas, which is known as the urban heat island (UHI) effect. UHIs occur because of the increased sensible heat flux from the land surface to the atmosphere near cities [2].

UHIs are often caused by compact and dense urban developments and low albedo coefficients of built-up materials, leading to high heat absorption by buildings [3]. Urban hard surfaces absorb heat during the day and radiate the heat overnight as infrared radiation. The extensive use of heat-absorbing materials for construction, reduced vegetative coverage, complex urban canyons and increased anthropogenic heat in metropolitan areas are some of the factors that contribute to the formation of UHIs [4–6]. UHI has adverse effects on human thermal comfort and energy demand of air conditioning [7]. One of the well-documented solutions to reduce the UHI effect in highly urbanised areas is the use of green infrastructure [8,9]. Therefore, the integration of green infrastructure into built-up areas has received considerable attention from researchers worldwide in recent years.

Green infrastructure has various types, including parks, street trees and green walls. The most feasible greening solution for highly urbanised areas is green roofs. Given that buildings occupy major land areas within the city and building roofs account for up to 32% of urban horizontal surfaces, the potential for retrofication is high. Vegetation and permeable soil used in green roofs help reduce the adverse effects of urbanisation on the local climate. Some cases have shown how unusable space located on rooftops can be successfully converted to contribute to sustainable cities [10].

* Corresponding author. Institute of Sustainable Industries and Liveable Cities, Victoria University, Australia.
E-mail address: elmira.jamei@vu.edu.au (E. Jamei).

https://doi.org/10.1016/j.buildenv.2023.110965
Received 22 May 2023; Received in revised form 28 September 2023; Accepted 20 October 2023
Available online 23 October 2023

Green roofs provide multiple benefits to ecosystems, buildings and urban areas. They increase the evapotranspiration rate in cities through their soil and plants, thereby redirecting the available energy to latent heat. Replacing conventional roofs with green roofs leads to reduced sensible heat for transmission to the air or building. Reducing energy use, mitigating UHI and improving outdoor thermal comfort are some effective strategies [11–14]. Relevant literature has indicated that green roofs also provide regulatory and cultural ecosystem services that safeguard public health [15]. The reduction in heat through green roofs is strongly linked to the reduction in cardiovascular diseases and death rates from mental disorders. Soumyajit et al. in their paper highlight that Green roofs not only contribute to improved air quality and temperature regulation but also provide a sustainable and aesthetically pleasing solution to urban and rural environmental challenges, further enhancing the overall well-being of local residents [16]. Asmaa et al. underscores the pivotal role of Urban Microclimate (UMC)-based models in addressing the complex interplay between urbanization, climate change, and public health. By conducting a thorough bibliometric analysis, we have illuminated the evolving landscape of UMC modelling and identified key areas of focus, including urban morphology and vegetation. It is evident that the research community is poised for further exploration of topics such as air quality, urban ventilation, and climate change within the UMC framework. This research serves as a roadmap for future investigations, highlighting opportunities for optimisation, data-driven approaches, and coupled models, all contributing to the ongoing paradigm shift in understanding and enhancing UMC performance [17]. Published literature shows that green roofs can help reduce UHI, cardiovascular disease mortality, mental illnesses and all-cause mortality in urban areas.

These benefits have motivated governments to develop legislation promoting the use of green roofs and provide incentives to pioneering stakeholders [18–20]. The Brisbane City Council has relaxed the specified maximum building height restriction for roof gardens provided that they are located in medium-to high-density residential, principal, major, district or mixed-use zones [21]. Similarly, in Toronto, Canada, the installation of a green roof space with 20%–60% of vegetation coverage has become mandatory for new structures with a roof area greater than 2000 m^2. Similar limits have been applied in Tokyo in Japan (20%), Portland in USA (70%) and Basel in Switzerland (15%) [18,19].

In Melbourne, the 'Green Our City Strategic Action Plan' aims to improve the quality and increase the quantity of greenery through partnerships with the industry and private sectors. The City of Melbourne owns less than one-third of the city's land area, and residents, businesses and the Victorian Government own more than two-thirds. Therefore, its four-year action plan (2017–2021) focuses on encouraging private sector participation in greening Melbourne.

'Green Our Rooftop, Treasury Place' is a project that is aligned with the objectives of the City of Melbourne's Green Our City Strategic Action Plan. The Treasury Place in Melbourne was selected for green roof implementation after an extensive process that included a public expression of interest and a thorough search to identify the most suitable site for the project. The building has the added benefit of being a high-profile site, which enables maximum exposure with regard to the promotion of the project. The site is well set up to complement the project's core objectives, including information sharing to inspire others to build their own green roofs. The proposed intensive green roof design is novel and unique because it represents the notion of 'Garden of Victorian Landscapes'. This green roof design is characterised by its unique 'topography' and 'bioregion' concepts and adopts a pixelisation approach in conjunction with a grid morphing algorithm to replicate the topography and bioregions of Victorian regions.

This study aims to quantify the effect of the proposed intensive green roof on UHI and thermal comfort at the Treasury Place (at rooftop and pedestrian levels) by using a numerical simulation tool (ENVI-met). This study also test number of design setting values (leaf area index [LAI], soil moisture, plant height and green coverage) to identify the optimum thermal performance of the proposed green roof. This study is important not only because it demonstrates the potential microclimate and human thermal benefits that a green roof can bring to the central business district (CBD) of Melbourne, but also because of the novelty of the design concept of the green roof, which is characterised by a diverse range of native plants across Victoria and situated on different topographies on the green roof, as well as the complexity in modelling the proposed green roof and the number of optimisation scenarios. This study is one of the first attempts to quantify the cooling potential and human thermal comfort benefits of a green roof with diverse plants and substrate depths. It addresses an important knowledge gap by proposing the most optimum design settings for a green roof in Melbourne, which has a temperate climate.

2. Literature review

By 2080, the maximum summertime air temperature will be 5.4 °C higher than that recorded between 1961 and 1990 [22]. Heat waves have also been increasing in intensity, duration and frequency, thereby exacerbating the heat-related mortality and morbidity rates across the globe [23]. People who live in urban areas are at high risks of increased temperature caused by the UHI effect. Local summertime air temperature can be reduced, and local UHI can be mitigated effectively by green infrastructure in cities [24–28]. However, there are limited areas in cities for green infrastructure. Approximately 30% of the horizontal areas in a city are building roofs, which offer valuable potential for adding vegetation for green infrastructure [28].

Green roofs are roof systems with live plants on top of the roofing membrane [29]. Green roofs are composed of different layers from the vegetation above to the substrate, water retention fabric, drainage layer, root barrier and roofing membrane below [30]. Green roofs are generally classified into two types: extensive green roofs (EGRs) that are mainly covered by sedum species with a maximum substrate depth of 150 mm and intensive green roofs (EGRs) with substrates more than 150 mm thick [31–33].

Many studies have been conducted on green roofs. In addition, extensive literature supports the fact that vegetation and greenery mitigate the UHI effect [34–39]. Plants have a cooling effect and can therefore be used strategically in urban and architectural design. The effects of green roofs on microclimate can be studied using various methods. These methods range from the multiscale phenomena method to observation and simulation techniques. The multiscale phenomena method is not always feasible due to the complexity of the UHI effect. Therefore, field measurements or simulation techniques are preferred.

One of the most frequently used tools to assess UHI is ENVI-met [40]. The model has high spatial resolution (0.5e10 m) and high temporal resolution (1e10 s), allowing users to assess the temperature of the canopy layer and thermal comfort, which vary greatly over short distances and periods [20]. Number of simulation -based studies have used ENVI-met to evaluate the impact of vegetation on urban microclimate [20,21,24,28,54]. ENVI-met has been mainly adopted to simulate surface–plant–air interactions in urban canyons and predict the climatic consequences of different urban design options [19–21]. Some studies have utilised ENVI-met to explore the climatic effects of green roofs at the building or neighbourhood scale [22,23]. However, in some cases, the lack of empirical data for verification increases the uncertainty of the simulation results.

ENVI-met has been used to assess the impact of seven green space scenarios at block and neighbourhood scales in Manchester, the UK, which has a temperate climate [41]. The findings of the simulation showed that even in suburban areas of temperate cities, just a 5% increase in green coverage can reduce the mean hourly surface temperature by 1 °C. Another simulation-based study that used ENVI-met revealed that dark-coloured conventional roofs with low albedos have high absorption of solar radiation and high surface temperatures (as high as 90 °C) on a summer day [42]. A comparison was made with a

Fig. 1. Treasury Place in Melbourne and its proposed green roof. (For interpretation of the references to colour in this figure legend, the reader is referred to the Web version of this article.)

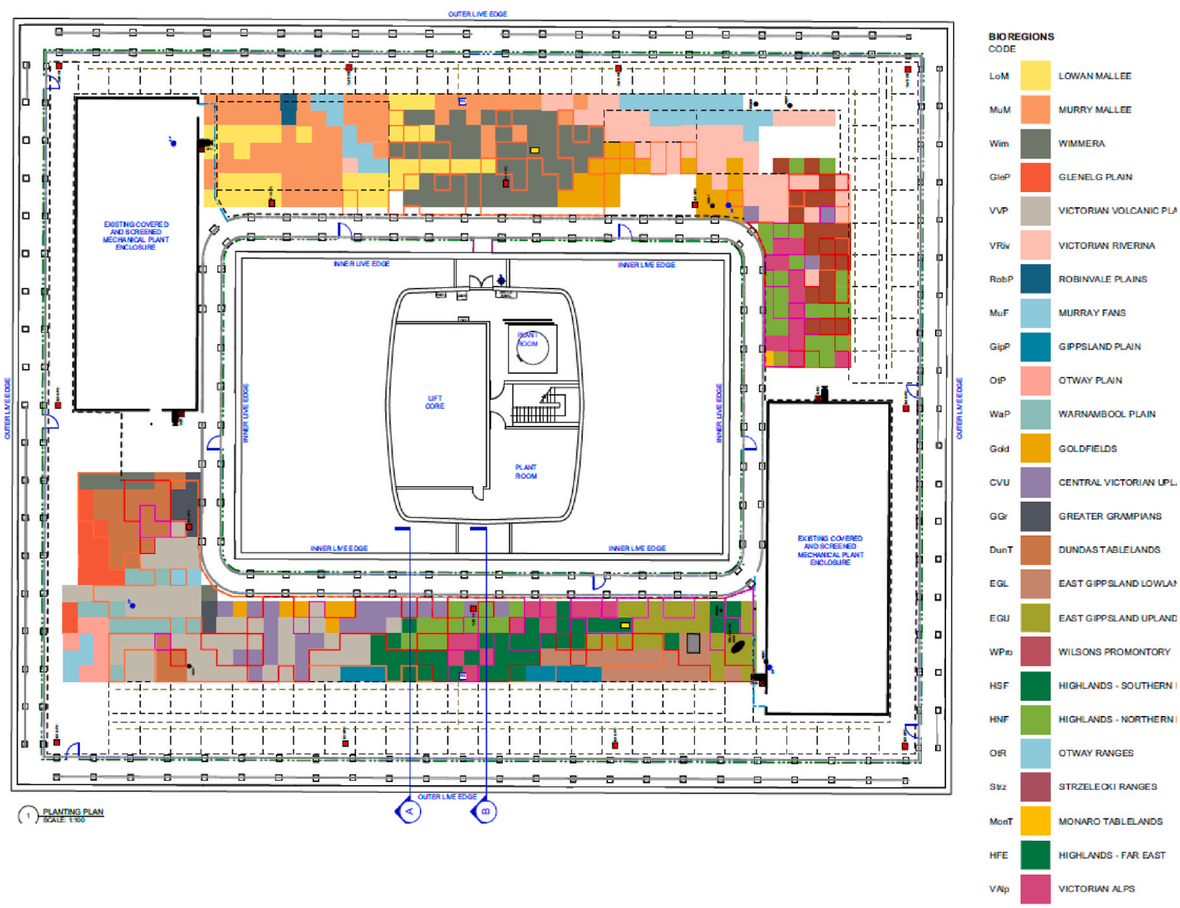

Fig. 2. Proposed bioregions for the Treasury Place's green roof. (For interpretation of the references to colour in this figure legend, the reader is referred to the Web version of this article.)

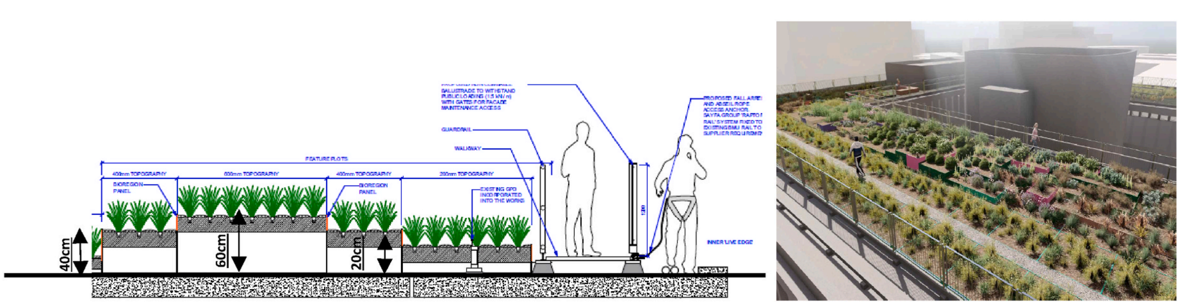

Fig. 3. Proposed topographies for the green roof that is abstracted at four different levels (0, 0.2, 0.4 and 0.6 m). (For interpretation of the references to colour in this figure legend, the reader is referred to the Web version of this article.)

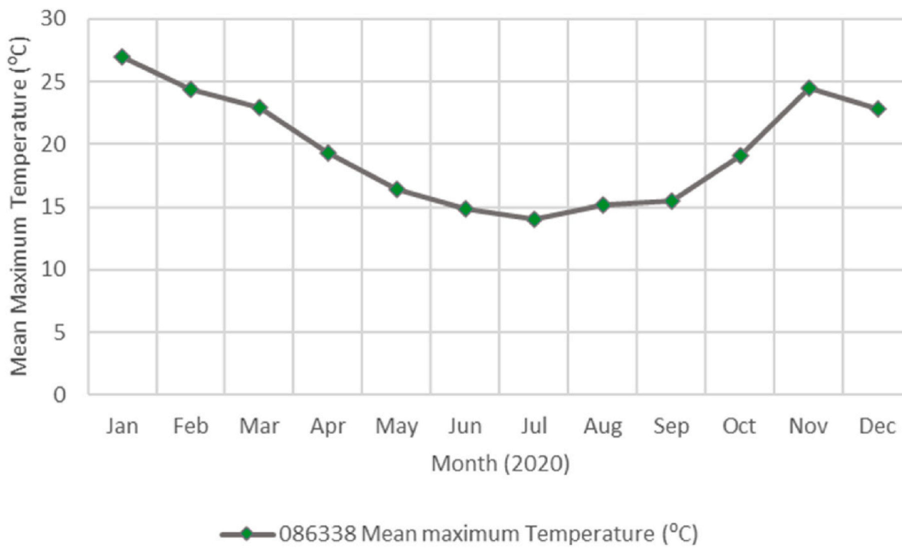

Fig. 4. Mean monthly maximum temperature in Melbourne (Olympic Park, station number 086338, 2013–present; source: BOM, Melbourne (Olympic Park), Victoria Weather Observation 2020).

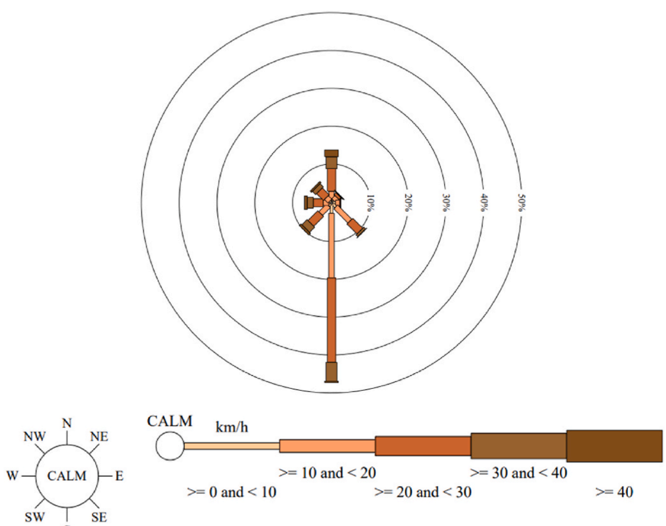

Fig. 5. Wind speed and direction in Melbourne (Olympic Park, station number: 086282) at 3 p.m. in summer (1 July 1970 to 9 August 2019) [68].

green roof scenario, where the heat received from the atmosphere and the surrounding air temperature were reduced through shading, surface reflection and evapotranspiration mechanisms. In actuality, shading and surface reflection reduce the energy load of a building and evapotranspiration, leading to evaporative cooling. As a result, green roofs become less warm during the day and contribute to low heat transfer to near-surface air.

Large-scale UHI studies have used mesoscale models to determine the cooling effects of vegetation. A study in Toronto quantified the cooling effect of green roofs at the city scale [43]. The results demonstrated that 50% green roof coverage (albedo is increased from 0.15 to 0.60) reduces the air temperature by 0.1 °C at 40 m above the ground level. City-wide green roof implementation has also shown promising results in mitigating UHI (0.3 °C-3 °C) [44]. Smith and Roeber found that the complete adoption of green roofs in Chicago has led to a 3 °C reduction in air temperature [45]. Similarly, the implementation of city-wide green roofs in New York has led to a 0.3 °C reduction in daily average temperatures and a 0.6 °C reduction in afternoon temperatures [46].

Green roofs provide different cooling effects at roof and pedestrian levels [34–39]. In Tokyo, Japan, the effect of green roofs on air temperature reduction was measured at the pedestrian level and found to be insignificant mainly due to the height of the surrounding buildings [47].

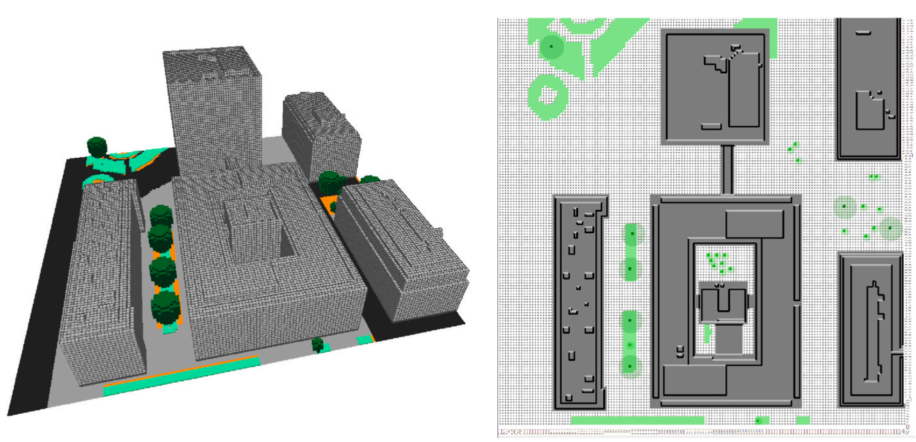

Fig. 6. Initial simulation base case scenario with no green roof (precinct scale). (For interpretation of the references to colour in this figure legend, the reader is referred to the Web version of this article.)

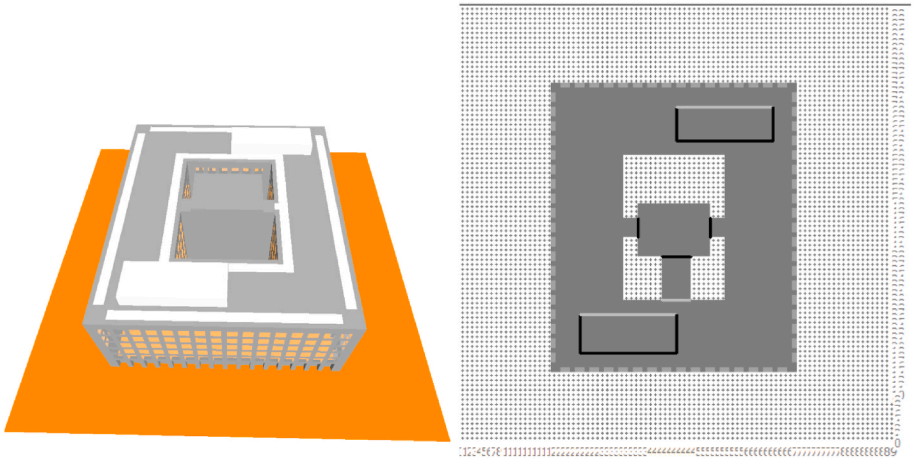

Fig. 7. Final simulation base case scenario with no green roof (building scale). (For interpretation of the references to colour in this figure legend, the reader is referred to the Web version of this article.)

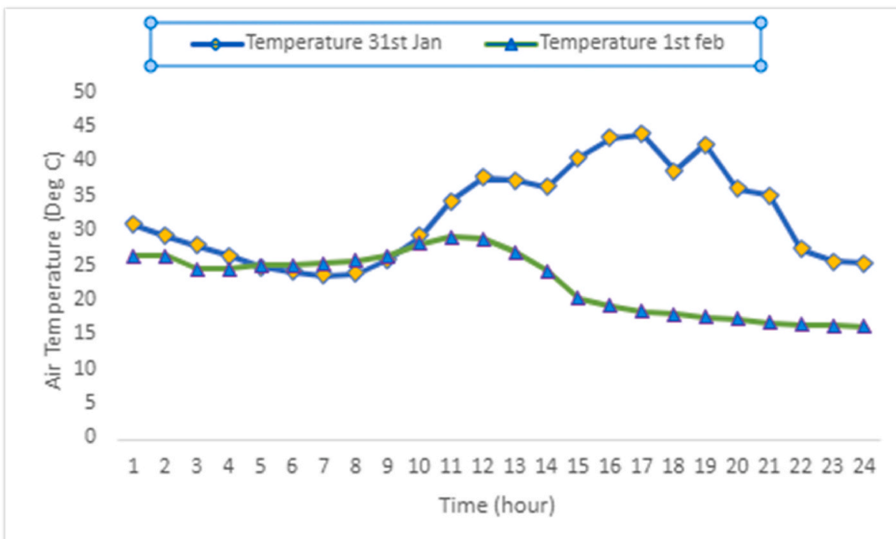

Fig. 8. Air temperature variation on 31 January and 1 February captured at the weather station installed at the Treasury Place's rooftop.
Source: weather station at roof top

Table 1
Overview of input data and parameter settings for the ENVI-met model.

Model parameter	Input value
Location	2 Treasury Place, East Melbourne VIC 3002
Model area	59 m × 50 m
Spatial resolution	Grid size: 90 × 90 x 40; dx = 1 m, dy = 1 m, dz = 1 m; dz of the lowest grid box is split into 5 subcells; model rotation out of grid north: −21.00
Simulation day	31 Jan 2020 and 1 Feb 2020
Simulation duration	31 Jan 2020 (6 a.m.) to 1 Feb 2020 (6 a.m.)
Simple forcing	Weather station data, air temperature and wind speed
Nesting grid	–
Sealed surfaces	Asphalt/concrete
Natural surfaces	Vegetation/sandy Soil

Similar results were obtained by Ng et al. for Hong Kong [48]. However, the use of extensive and intensive green roofs in low-rise buildings in Hong Kong reduces the pedestrian-level air temperature by 0.4 °C-0.7 °C and 0.5 °C-1.7 °C, respectively [49]. Lazzarin et al. compared the thermal effects of green roofs in wet and dry Italian temperate climates by using field measurements and numerical simulations. The results showed that the surface temperature is 55.8 °C and 40 °C under dry and wet conditions, respectively [50]. Other recent urban studies have revealed that the combined effects of leaf shading, albedo, humidity and thermal mass determine the cooling capacity of green roofs [51]. For example, a study in Neubrandenburg, Germany, assessed the cooling effects of green roofs before and after rain; the results showed that the substrate of green roofs exhibits a temperature difference of 5 °C under wet and dry conditions [52].

Meanwhile, a study conducted in the CBD of Melbourne investigated the microclimate and human thermal comfort effects of green roofs by using ENVI-met [53]. The simulation results suggested that green roofs in high-rise buildings can lead to 0.47 °C and 0.27 °C reductions in the air temperature in the surrounding area. A similar simulation-based study in the City of Melbourne reported that increasing the green roof coverage from 30% to 90% reduces the maximum roof surface UHI from 1 °C to 3 °C and improves human thermal comfort by 4 °C [54]. The cooling potential of green roofs depends on several variables, such as roof type, soil moisture and plant features (e.g. plant height, LAI and plant coverage/type) [55]. Santamouris showed that the cooling potential of green roofs also relies on the roof U value, latent heat loss and

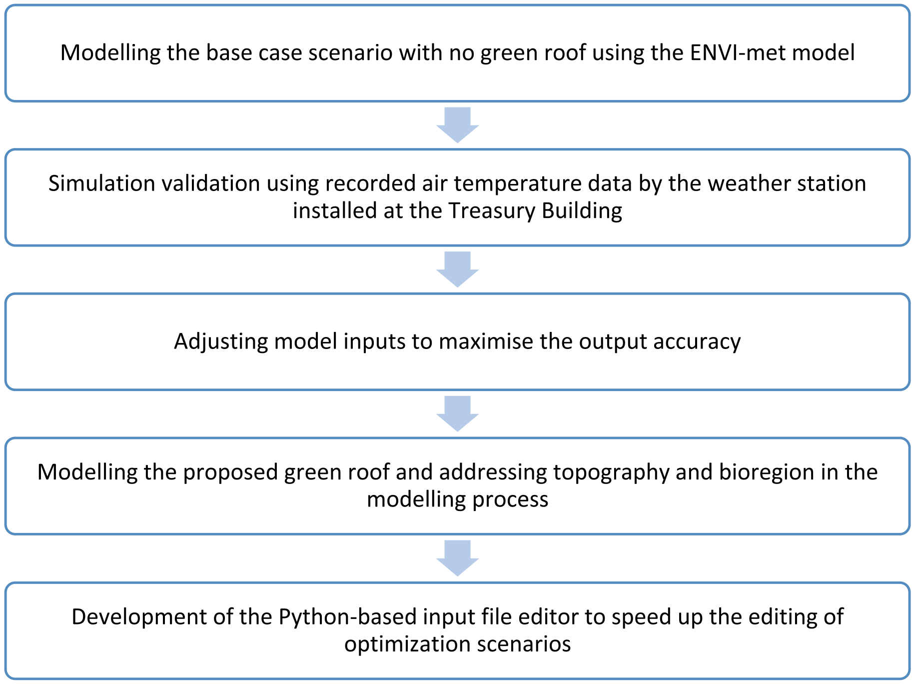

Fig. 9. Step-by step modelling process of the proposed green roof in ENVI-met. (For interpretation of the references to colour in this figure legend, the reader is referred to the Web version of this article.)

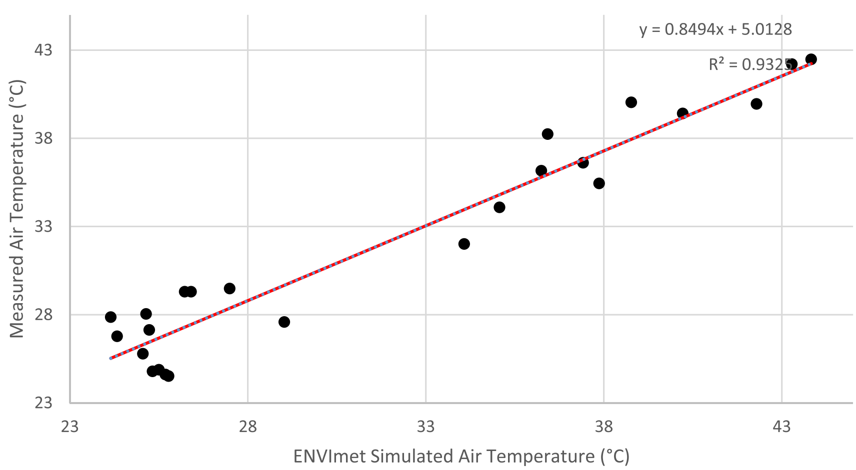

Fig. 10. Relationship between ENVI-met simulation and weather station air temperature monitoring records on 31 January 2020 ($R^2 = 0.93$).

local climatic context [5].

A study in the warm, humid climate of Hong Kong revealed that plant type, form and biomass structure are key parameters that affect the thermal performance of green roofs [56]. In a similar study, Zeng identified the optimal parameter setting for green roofs in different climate zones of China and concluded that LAI is the main parameter that influences the energy performance of green roofs in cooling-dominated areas [57]. The thermal performance of green roofs in South Australia is mainly governed by LAI, albedo and the insulative values and depth of the substrate [58]. Stomata resistance and water availability of the substrate have insignificant effects on thermal performance.

The cooling potential of green roofs also depends on the geographic and climatic backgrounds of the study area. According to a systematic literature review [59], the potential cooling effect of green roofs is strongly influenced by the geographic and climatic conditions of the selected site. This study also identified some of the key barriers in implementing green infrastructures at small and large scales (e.g. lack of coordination across different levels of government, lack of financial incentives for stakeholders, irrigation and maintenance costs).

Green roofs reduce the surface temperature of buildings. A study by Feng Chi demonstrated that green roofs decrease the surface temperature by up to 30 °C [60]. However, the capacity of a building to reduce near-surface and surface air temperatures depends on green roof structural design parameters. Several studies have shown that the insulation layer plays an important role in maximising the thermal and energy performance of green roofs [61,62]. A study in Melbourne quantified the insulation value of three substrates (scoria, bottom ash and crushed roof tiles) under three humid conditions. Compared with 100-mm-thick scoria substrates, wet ones have R values ranging from 0.3 (wet) to 0.8 (dry) and the highest air-filled porosity and lowest humidity content [63]. Green roofs, especially those with large depths and good

Table 2
LAI, plant height, soil moisture and tree coverage values in the optimisation scenarios.

‘	Optimised Value	Optimisation Scenario
LAI (m^2/m^2)	0.69 (average LAI of the proposed green roof)	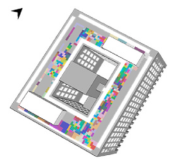
	1.08	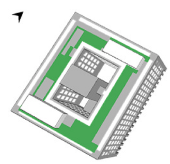
	2.5	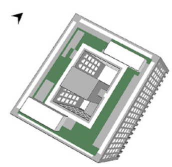
Plant height (m)	0.2	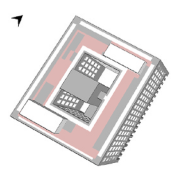
	0.33 (average plant height of the proposed green roof)	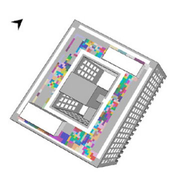
	0.4	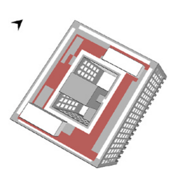
	0.6	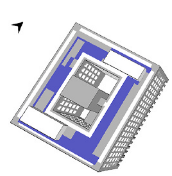
Soil moisture [0.1] (bars)	0.1	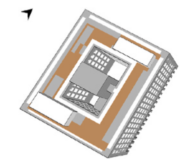
	0.3	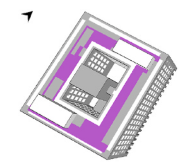
	0.5 (default soil moisture of the proposed green roof)	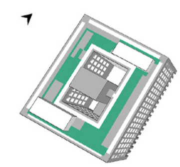
	0.6	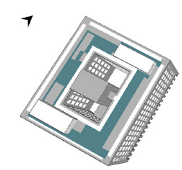
Increase tree coverage (%)	+50%	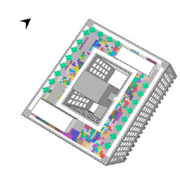

moderation of temperature fluctuation, also delay heat transmission through buildings with a 4–8 h lag [58]. However, green roofs with more than 150 mm depth in South Australia lead to a small thermal benefit [64].

Plant type is another key element that affects green roofs' cooling impact. The effect of plant type on the thermal performance of green roofs has been evaluated using different combinations of monocultures and mixtures of three drought-tolerant high-water-use species (*Lomandra longifolia*, *Dianella admixta* and *Stypandra glauca*) [65]. The results showed that in summer, the mixture cools better than all monocultures, except for *L. longifolia*, thus reducing the substrate temperature through evapotranspiration and improving the substrate's insulation benefits. Future research should focus on the effects of various plant species on green roof thermal benefits because only a limited number of species have been studied [65].

The current study aims to quantify the effect of the proposed intensive green roof on UHI and thermal comfort in the Treasury Place (at rooftop and pedestrian levels) by using a numerical simulation tool (ENVI-met) and recommends optimal design settings that can further improve green roof thermal performance. Treasury Place is a prominent governmental building in a prime location in the CBD of Melbourne. Public buildings serve as examples in this pursuit because enhancing energy efficiency within these structures is pivotal in societies' proactive responses to multifaceted challenges, such as climate change, economic

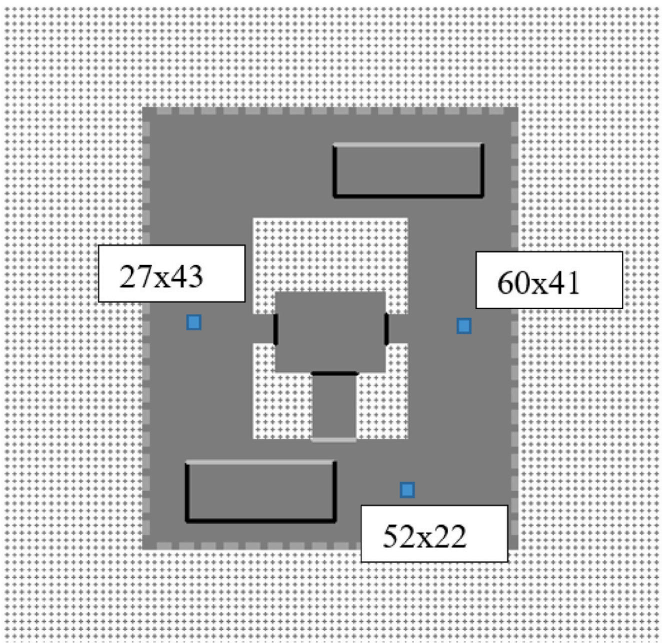

Fig. 11. Locations of receptors positioned at the rooftop in the ENVI-met area input file.

advancement and energy security. Consequently, the enhancement of energy efficiency standards for public buildings to foster a concomitant reduction in the UHI effect has become a foundational strategy nationally and internationally. This strategy promotes environmentally conscious construction and yields reduced energy consumption and associated emissions, thereby producing notable economic gains, and community awareness.

In the context of the UHI effect, which detrimentally influences energy usage within buildings, promotion of the use of green roofs has emerged as a paramount objective in energy policies at regional, national and global fronts. The prevailing issue of elevated energy consumption coupled with subpar energy efficiency in public buildings is a major concern and underscores the substantial untapped potential of energy conservation.

In the following section, a brief overview of the study area is provided, and the green roof design concept, the method used to quantify the cooling impact of the proposed green roof and the optimisation scenarios are discussed.

3. Methodology

3.1. Study site and green roof design concept

The Treasury Place is also called the State Government Office in Melbourne and was built in the 1960s with five levels of office spaces accommodating the Department of Treasury and Finance (DTF) and the Victorian Government Department of Premier and Cabinet (DPC). Fig. 1 shows aerial photos of the Treasury Place and the location of the proposed green roof.

The purpose of retrofitting the Treasury Place is to demonstrate how green roofs can be successfully retrofitted on an existing building and to break down perceived barriers to green roof retrofitting among stakeholders and communities. The 'Green Our Rooftop' project is based on the notion of 'Garden of Victorian Landscapes' and aims to apply research-based design principles to trial and test conditions to continue learning and developing the science of green roofs in Melbourne, Australia. It also aims to provide a place for learning that will facilitate green roof promotion and for viewing, learning and sharing information about the best practice of green roofs.

The design concept of the proposed green roof of the Treasury Place is based on the diversity of Victorian plant types (bioregions) and Victorian plain's topography. Through the use of pixelisation and grid morphing techniques, such diversity is reflected in the design of the green roof and captured by the green roof plan through the introduction of so-called 'bioregions' (Fig. 2) and the positioning of these bioregions at different heights (to demonstrate Victorian topography) (Fig. 3). The green roof designer and landscape architect team considered the elevation from the sea level across the state and abstracted the entire topography into four different heights from the green roof (0, 0.2, 0.4

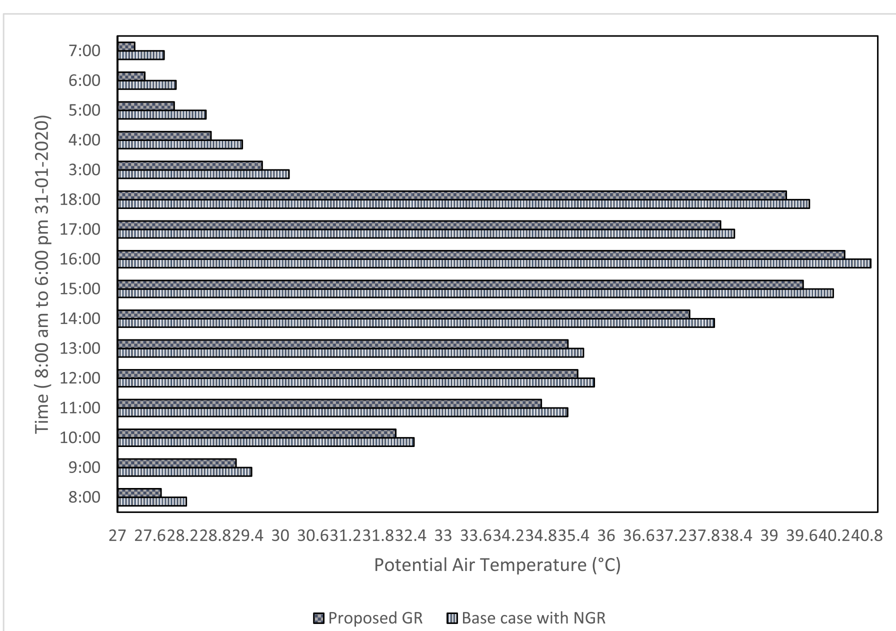

Fig. 12. Comparison of air temperature values in the base case scenario with no green roof and the proposed green roof scenario on the hottest day (31 January 2020) captured at a height of 1.5 m from the roof. (For interpretation of the references to colour in this figure legend, the reader is referred to the Web version of this article.)

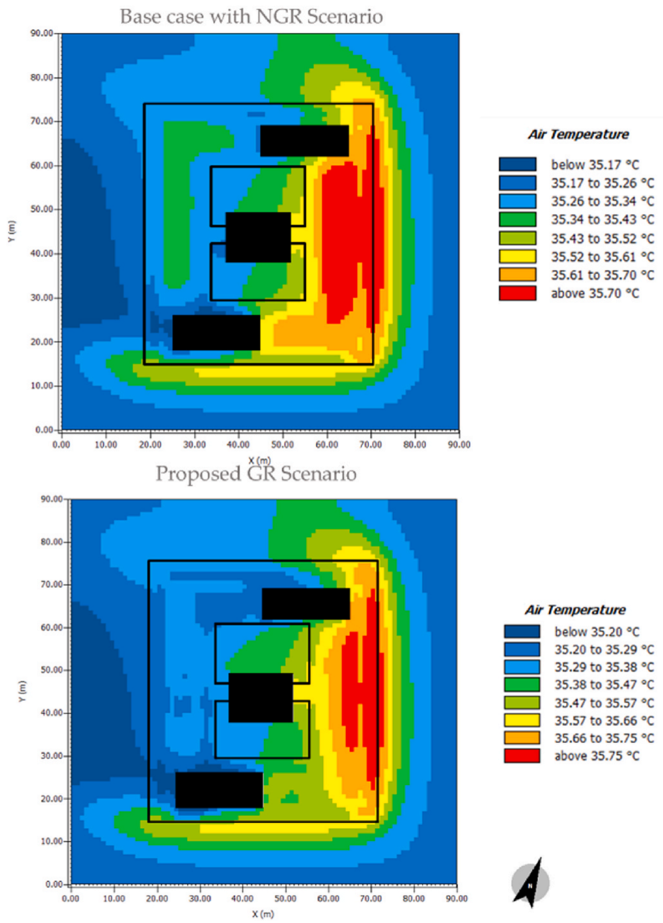

Fig. 13. Air temperature spatial distributions in the base case scenario with no green roof (top) and proposed green roof scenario (bottom) captured at 1.5 m from the roof. (For interpretation of the references to colour in this figure legend, the reader is referred to the Web version of this article.)

and 0.6 m). Additionally, Victoria's topography is represented with 200 mm height increments by stepping the garden edge restraints set onto void formers. The layout of these stepped plots is determined by an abstraction of Victoria's topography pixelated and transposed onto feature plots (1 m × 1 m grid). As a result, the proposed green roof consists of bioregion areas that are low and flat (e.g. Mallee and Western Plains) and areas that are undulating and high (e.g. the Great Dividing Ranges, Gold Field Ranges, Grampians, Otway Ranges and Gippsland Highlands).

The concept design of the green roof demonstrates the diversity of Victorian plant types through a colour-coded bioregion reflected in the design of the green roof (Fig. 2). The bioregions are mapped on the grid of the roof in the same pixelated and transposed manner as topography. Each of the 1 m × 1 m plots is planted with species that represent a certain bioregion. Each bioregion in the concept plan represents a landscape typology within the state.

3.2. Climate condition

According to the Köppen climate classification, Melbourne has a temperate oceanic climate with hot summers (typically from December to February) with 25.3 °C mean monthly maximum temperature and 40 °C maximum temperature in summer [66]. Melbourne experiences elevated summer temperatures due to the UHI effect, which makes it vulnerable to heatwaves. During such events, the well-being of urban populations can be severely compromised. A notable instance is the Black Friday heatwave in late January 2009, which lasted for three days and led to an alarming increase of 374 deaths in Victoria, Australia, compared with usual circumstances. Annually, Melbourne encounters an average of nine scorching days with temperatures exceeding 35 °C. However, projections indicate a worrisome situation: this count is anticipated to increase to 11 days by 2030 and to 20 days by 2070. These predictions are based on climate change models developed by the Bureau of Meteorology (BOM) and the Commonwealth Scientific and Industrial Research Organisation, both of which suggest a mounting trend in extreme heat days in the coming years. Such projections hint at the highest possibility of extended heat exposure during heatwaves further exacerbated by the UHI effect. In summary, Melbourne's susceptibility to elevated temperatures and increasing occurrences of heatwaves, combined with the amplifying influence of UHI, underscores the

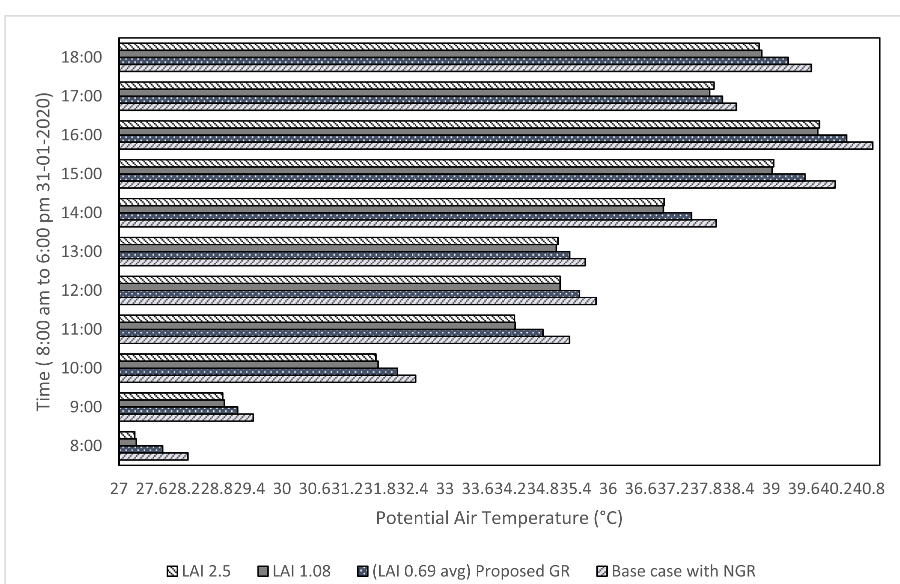

Fig. 14. Comparison of air temperature values between the base case scenario with no green roof, the proposed green roof scenario and optimised LAI scenarios (1.8 and 2.5) on 31 January 2020 captured at 1.5 m from the roof. (For interpretation of the references to colour in this figure legend, the reader is referred to the Web version of this article.)

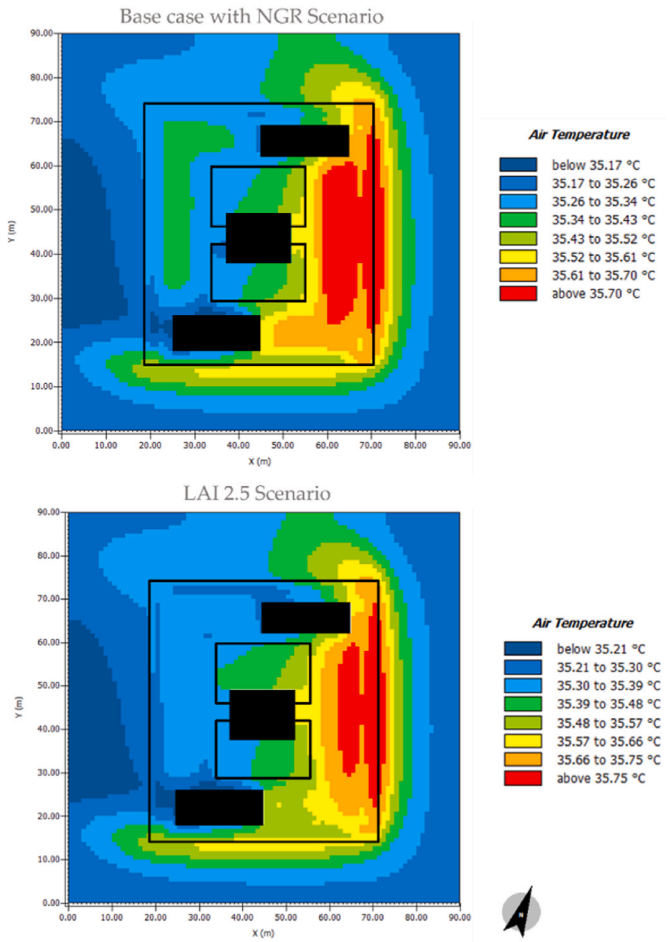

Fig. 15. Air temperature spatial distributions in the base case scenario with no green roof (top) and optimisation scenario 1 with LAI = 2.5 (bottom) captured at 1.5 m from the roof. (For interpretation of the references to colour in this figure legend, the reader is referred to the Web version of this article.)

escalating risks posed by extreme heat events to public health and the need for effective mitigation strategies. Therefore, in this study, we selected the warmest day in the year to mimic the worse-case (heatwave) scenario and assess the maximum potential cooling benefits that can be achieved by installing the proposed green roof.

Fig. 4 shows the mean maximum temperature distribution in 2020 obtained from the Melbourne Olympic Park Station (Location: 086338). According to Fig. 4, January was the hottest month. It was selected as the date to conduct the simulations and field measurements so that the worst-case scenario with the highest level of urban air temperature and thermal distress was considered.

The variation in wind speed depends on the time and season. Wind speed is normally the lowest during nighttime and in the early morning before sunrise. Given that surface heat induces turbulence, wind speed increases during the day. Wind speed is also affected by weather phenomena, including showers and thunderstorms. Early spring and late winter have extremely windy days. On 3 September 1982, a strong wind gust of 120 km/h was recorded [67]. Fig. 5 illustrates the wind direction and speed at Olympic Park in Melbourne at 3 p.m. in summer.

The climatic data in this study were derived from the nearest BOM to the site and a weather station that was installed on the top of the Treasury Place to monitor the local climatic parameters, including air temperature (°C), relative humidity (%), solar radiation (W/m^2) and wind speed (m/s) at the local scale. The recorded data were then inputted to the ENVI-met model to validate the simulation outputs.

3.3. Method

The methodology of the study involved numerical simulations and verification via field data collection. The simulations were conducted with ENVI-met v4.2, a 3D microclimate simulation software. The use of ENVI-met v4.2 is appropriate for the purpose of this study because this software was developed to evaluate outdoor thermal comfort conditions with respect to pollution dispersion and indoor climate, the microclimatic effects of urban structures and the green element effects on meteorological parameters [69]. Version 4.2 of ENVI-met has been considerably improved, particularly in terms of the generation of sophisticated vegetation profiles with the Albero database [70,71], and has been positively validated in a number of cities worldwide [72,73]. After simulation, various thermal comfort indices, such as the Universal Thermal Comfort Index (UTCI) and the Physiologically Equivalent Temperature (PET) Index, can be calculated with the BioMet tool. German guidelines for assessing the perceived heat sensation of pedestrians have recommended the use of the PET index and categorised it into nine classes of thermal stress ranging from extreme heat stress (>41 °C) and comfortable thermal conditions (18 °C-23 °C) to extreme cold stress (<4 °C) [74–76]. Therefore, in this study, the PET index was used.

3.3.1. Modelling base case scenario (no green roof)

The model domain of the site was digitalised using an aerial photograph extracted from Google Earth (Fig. 6). The site was rotated 21° from the grid north (counter-clockwise) to align the model with the actual north. The initial modelled site covered an area of 59 m × 50 m. The size of the grid for modelling the site was 90 m × 90 m × 40 m to avoid errors during the simulation and reduce the computation time. Fig. 7 shows the building scale of the final model in ENVI-met with 1 m spatial resolution (see Fig. 8).

The simulation began from 6 a.m. on 31 January 2020 to 6 a.m. on 1 February 2020 because this period is the hottest time of the year in Melbourne. The recorded data from the weather station at the Treasury Place's rooftop were used as an input to the ENVI-met model. Simple forcing (12 a.m.–12 p.m. cycle) was used to mimic the existing climatic condition around the building.

Building information (e.g. height, material) was obtained from architectural drawings provided by the City of Melbourne. Table 1 presents an overview of the input settings of ENVI-met utilised to initiate the base case scenario simulation. The weather forcing data and project-specific database file were located in the configuration file and used to run the model.

3.3.1.1. Validation against field measurements. The influence of greening on the thermal comfort of buildings has been thoroughly investigated using the ENVI-met software package in various studies conducted across the world [48,77,78]. All modelling systems must be validated against field measurements to determine their ability to produce accurate outputs within the urban environment. Therefore, field measurements were conducted in this study to validate the simulated outputs against the recorded data. Field measurements were used to verify ENVI-met. A weather station was installed on top of the Treasury Place to monitor meteorological conditions. The weather station was mounted 90 m above the ground and collected local climatic conditions, such as air temperature, relative humidity, wind speed and radiation.

For the objective of this study, the hottest day in 2020 (31 January 2020) was selected. The air temperatures simulated and recorded by the weather station on the exact day were extracted and compared. Fig. 10 shows the correlation values between the simulated and measured air temperatures. The ENVI-met simulation and measured results showed reasonable agreement, with an R square of 0.93. The accuracy of ENVI-met in modelling the air temperature variation at the Treasury Place for summer courses was confirmed by the verification results of onsite long-

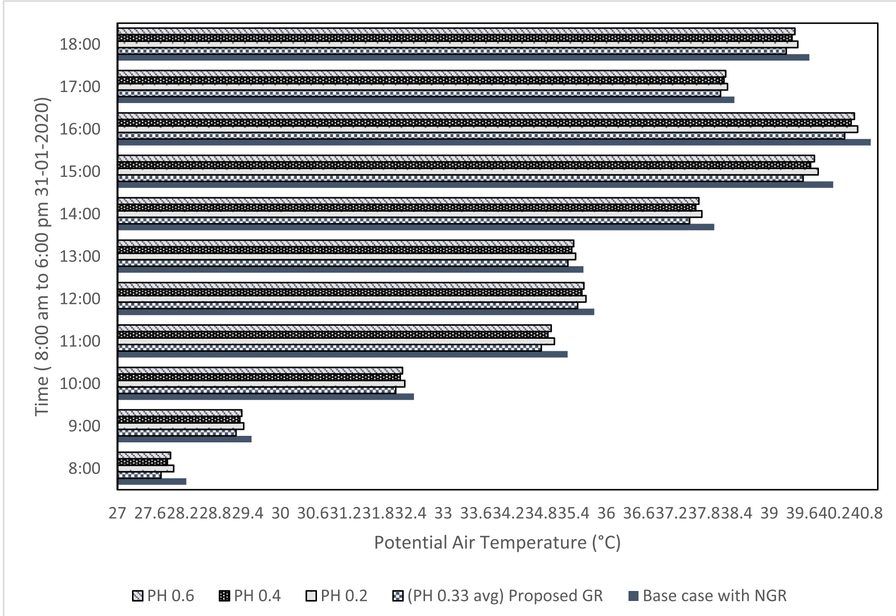

Fig. 16. Comparison of air temperature values between the base case scenario with no green roof, the proposed green roof scenario and optimisation scenario 2 with the mean plant height set to 2, 0.4 and 0.6 on 31 January 2020 captured at 1.5 m from the roof. (For interpretation of the references to colour in this figure legend, the reader is referred to the Web version of this article.)

term monitoring.

ENVI-met does not individually consider the influence of anthropogenic heat on air temperature. Given the highly dense and massive building structures prevalent in many areas, the potential impact of human-generated heat can be viewed as a constant factor that contributes to the difference between observed and simulated air temperature values. This interpretation aligns with the common use of ENVI-met in simulating outdoor air temperatures in studies related to urban climatology [20,28,46,56]. Once ENVI-met and its input settings were verified in the current work, simulations of the proposed green roof and optimisation scenarios were initiated.

3.3.2. Modelling the proposed green roof scenario

One of the important challenges in modelling the proposed green roof was embedding the design concept (which relied heavily on bioregions and topography) into the simulations. Sixty-seven plant types were generated in ENVI-met by modifying the specifications of existing plants in terms of height, albedo, root zone, depth, LAI and root area density to model the bioregions. Each plant information was stored in the.ebd file format. The Python-based.ebd file editor tool was developed for editing the project-specific.ebd file dynamically to model the proposed green roof efficiently.

The simulated green roof had 350 plantation regions and 67 plant types. The custom Python-based script editing tool allowed these parameters to be edited at a high rate during the optimisation scenarios. Conventionally, the user interface in ENVI-met is used to edit vegetation features; however, due to the large number of plant types and the complex nature of the proposed green roof, the Python-based.ebd file editor was developed and used in this project to enable an efficient simulation. The proposed plants were modelled, and the air gap between the substrate and the wall was considered to mimic topographies in the proposed green roof design.

Air gaps have been previously used in Ref. [79] to demonstrate the topography employed in the simulation of a green roof. In an experimental study conducted in Sydney [79], the thermal benefits of installing a green roof on a timber-framed building were quantified. The results showed the improved thermal performance of the green roof as a result of the high thermal insulation characteristic caused by the existing air layer trapped inside the timber-framed structure. Fig. 9 illustrates the step-by-step modelling process of the proposed green roof in ENVI-met.

3.3.3. Modelling optimisation scenarios

Four optimisation scenarios were modelled to examine whether the proposed green roof's cooling potential can be further maximised. These scenarios included (1) increasing LAI values, (2) varying plant height, (3) increasing soil moisture and (4) adding tree coverage (50%) to the proposed green roof. Table 2 presents the values of LAI, plant height, soil moisture and tree coverage used in each optimisation scenario. Notably, all other input parameters were kept constant with the proposed green roof scenario to facilitate the comparison of optimisation scenarios. The input files for each optimisation scenario were generated using the custom.ebd file editor.

4. Results and discussion

This section presents the simulation results and highlights the cooling effect of each scenario at the rooftop and pedestrian levels in (1) the existing scenario with no green roof, (2) proposed green roof scenario and (3) the suggested optimisation scenarios outlined in the Methodology Section. In this study, the cooling effect was defined as 'the air temperature difference between the base case and proposed green roof scenarios' and 'the air temperature difference between the proposed green roof and optimisation scenarios'.

The cooling effect was evaluated during daytime from 6 a.m. to 6 p.m. at rooftop (1.5 m above the roof surface) and pedestrian (1.5 m from the ground level) levels. Three receptors were positioned at rooftop and pedestrian levels to extract the mean air temperature values. Fig. 11 shows the location of the receptors at the rooftop level.

Fig. 12 presents the air temperature comparison between the base case scenario and the proposed green roof scenario at the rooftop level. According to Fig. 12, an average reduction of 0.2 °C and a maximum reduction of 0.7 °C were obtained after installing the proposed green roof. The minimum cooling impact was observed at 11 a.m., with a 0.1 °C air temperature reduction. Fig. 13 shows the air temperature spatial distribution in the base case scenario with no green roof and in the proposed green roof scenario. The results of the simulations are in

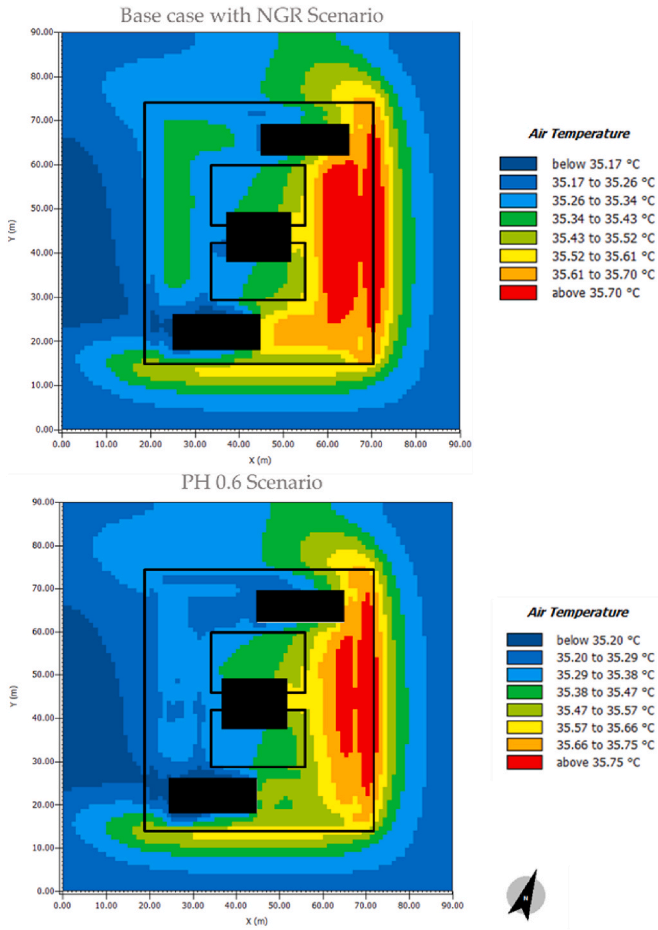

Fig. 17. Air temperature spatial distributions in the base case scenario with no green roof (top) and optimisation scenario with increased mean plant height = 0.6 m (bottom) captured at 1.5 m from the roof. (For interpretation of the references to colour in this figure legend, the reader is referred to the Web version of this article.)

line with those of [80], which showed that green roofs reduce the air temperature by 0.1 °C-0.3 °C. Similar findings were reported in Ref. [81], which revealed that green roofs can contribute to reduced temperatures in high-density urban areas. Similarly [82], showed that green roofs in Nanjing reduce roof-level air in low/midrise buildings by up to 0.35 °C-0.45 °C.

As shown in Fig. 13, the LEONARDO images exhibited a clear reduction in red and orange zones, indicating few areas with high air temperatures.

4.1. Optimisation scenario 1: increased LAI

In the first optimisation scenario, various LAIs were tested to identify the optimum LAI that leads to the maximum cooling impact. The mean LAI value in the proposed green roof scenario was 0.6, which was increased to 1.08 and 2.5 to maximise the cooling effect in the proposed green roof scenario.

Fig. 14 shows the mean values of air temperature in the base case scenario, proposed green roof scenario (increased LAI to 1.08) and optimisation scenario 1 (increased LAI to 2.5). An average reduction of 0.8 °C in air temperature was recorded after increasing LAI to 1.08. The cooling effect reached its maximum (1.5 °C) at 10 p.m. in this scenario. The minimum cooling effect (0.47 °C) was reported at 7 pm.

When LAI was increased to 2.5, further reduction in the mean air temperature values was observed. However, the magnitude of reduction in air temperature was not significant, which can be mainly explained by the evapotranspiration limitation of the mathematical model used in ENVI-met. The maximum air temperature difference between the base case scenario with no green roof and optimisation scenario 1 (with increased LAI to 2.5) was as high as 1.5 °C. The minimum cooling impact (0.31 °C) was recorded at 7 pm.

According to Fig. 14, increasing the LAI in the proposed green roof scenario to 1.8 and 2.5 resulted in further reduction in the air temperature values. However, high values of LAI did not always contribute to improved thermal performance during the testing of the impact of high LAI values on the cooling effect of the green roof. This situation can be explained by the restriction in airflow within the green canopies, leading to an increased air temperature around the green areas.

Fig. 15 shows the spatial distributions of air temperature in the base case scenario with no green roof and optimisation scenario 1 with LAI of 2.5. The increased coverage of the blue zones and the reduction in the red zones near the built-up areas confirmed the effectiveness of optimisation scenario 1 in reducing the air temperature and mitigating UHI at the rooftop level.

4.2. Optimisation scenario 2: increased plant height

In the second optimisation scenario, the average plant height was increased to 0.2, 0.4 and 0.6 m. A series of trials was performed to determine the values that lead to the maximum cooling impact in comparison with the proposed green roof scenario. The mean plant height value for the proposed green roof was calculated to be 0.3 m. The average plant height was increased three times to quantify the cooling impact. Fig. 16 shows the mean values of air temperature for the base case scenario, proposed green roof scenario and optimisation scenario 2.

Fig. 16 shows the mean plant height that was increased from 0.3 m (in the proposed green roof scenario) to 0.2, 0.4 and 0.6 m in optimisation scenario 2. As shown in Fig. 16, the average air temperature across the green roof decreased. When the mean plant height value was increased to 0.2 m, the maximum cooling impact was achieved, and the air temperature at the rooftop level was reduced by 0.3 °C in the late afternoon. The lowest cooling effect was reported at 7 a.m., and the air temperature decreased by only 0.05 °C. When the mean plant height value was increased from 0.2 m to 0.4 m, the thermal performance of the proposed green roof improved, and the maximum cooling impact was achieved in early evening, with a 0.5 °C reduction in the average air temperature at the roof level. The green roof's lowest cooling potential was reported in early morning, and the air temperature was reduced by 0.075 °C.

When the mean plant height value was increased from 0.4 m to 0.6 m, the rooftop-level average air temperature increased slightly. However, the thermal performance of the proposed green roof still improved because the average air temperature was reduced by 0.4 °C in this scenario. The minimum cooling effect in this scenario was also reduced, with only a 0.0625 °C decrease in air temperature, which was slightly lower than the 0.075 °C air temperature reduction when the mean plant height was set to 0.4 m.

Fig. 17 shows the air temperature spatial distributions in the base case scenario with no green roof and optimisation scenario 2 with 0.6 m mean plant height. The coverage of the blue zones increased, and the red zones near the buildings were reduced. The effectiveness of the proposed optimisation scenario was confirmed when plant height was set at 0.6 m.

4.3. Optimisation scenario 3: increased soil moisture

In the third optimisation scenario, the soil moisture in the existing scenario (0.5) was increased to 0.1, 0.3 and 0.6 after conducting a series of trials to determine the optimum values that maximise the cooling potential of the proposed green roof. The air temperatures in the base case scenario with no green roof, proposed green roof scenario and optimisation scenario 3 (increased soil moisture) were compared to quantify the effect of increased soil moisture on air temperature.

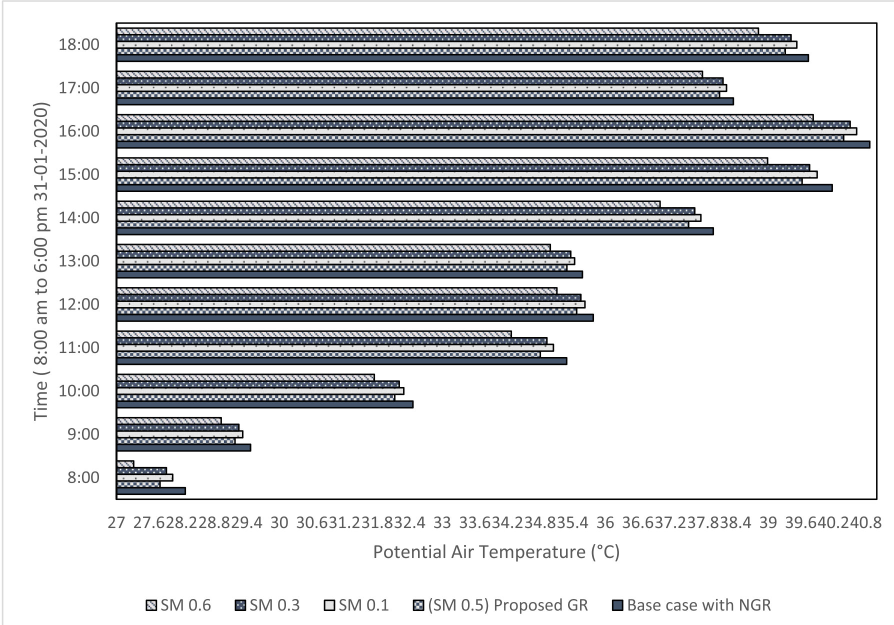

Fig. 18. Comparison of air temperature values in the base case scenario with no green roof, proposed green roof scenario and optimised soil moisture scenarios (0.1, 0.3 and 0.6) on 31 January 2020 captured at a height of 1.5 m from the roof. (For interpretation of the references to colour in this figure legend, the reader is referred to the Web version of this article.)

When the soil moisture was increased to 0.1, the maximum cooling impact decreased by 0.3 °C in the early evening. This value increased to 0.5 °C and 1.5 °C when the soil moisture was further increased to 0.3 and 0.6, respectively. The least cooling effect for optimisation scenario 3 was observed in the early morning. Increasing the soil moisture to 0.1, 0.3 and 0.6 resulted in 0.1 °C, 0.3 °C and 0.5 °C reductions in the average air temperature across the green roof.

Fig. 18 shows the variations of air temperature in the base case scenario, the proposed green roof scenario and optimisation scenario 3. Increasing the soil moisture from 0.5 in the proposed green roof scenario to 0.6 in optimisation scenario 3 resulted in a substantial improvement in the green roof's cooling potential.

Fig. 19 shows the air temperature spatial distributions at the rooftop level for the base case scenario, proposed green roof scenario and optimisation scenario 3 with different soil moisture values (0.1, 0.3 and 0.6). The increased coverage of the blue zones and the reduction in the red zones near the buildings confirmed the effectiveness of optimisation scenario 3. The best thermal performance was achieved when soil moisture was set to 0.6, and the lowest thermal performance was recorded when the soil moisture was set to 0.3 and 0.1. When soil moisture increased, the reduction coefficient of air temperature also increased. The reduction in air temperature was directly proportional to the increase in soil moisture but was limited by evapotranspiration, as discussed in the previous sections. In the impact analysis, the soil moisture of the baseline model was set to 0.5.

4.4. Optimisation scenario 4: adding tree coverage

In the fourth optimisation scenario, tree coverage was included in the simulation, and 50% of the proposed green roof was replaced by trees to determine if the cooling impact can be further improved. Fig. 20 shows the air temperature variation in the base case scenario with no green roof, proposed green roof scenario and optimisation scenario 4. Optimisation scenario 4 contributed a mean reduction of 0.05 °C across the green roof. The maximum cooling effect in this scenario was observed at noon time, with the average air temperature being reduced by 1.03 °C. The least cooling effect reported in this scenario was captured at 12 p.m., with a 0.22 °C drop in the mean air temperature.

Fig. 21 shows the air temperature spatial distributions in the base case scenario, proposed green roof scenario and optimisation scenario 4. The increased coverage of the blue zones and the reduction in the red zones near the buildings confirmed the effectiveness of optimisation scenario 4 at the rooftop level.

5. Comparative analysis

This section provides a comparative analysis of the impact of each optimisation scenario on the cooling performance of the proposed green roof. Table 3 shows the maximum cooling impact values were from optimisation scenario 1 (increased LAI to 2.5), optimisation scenario 2 (increased plant height to 0.3), optimisation scenario 3 (increased soil moisture to 0.6) and optimisation scenario 4 (adding 50% tree coverage). The optimum values in each optimisation scenario were extracted and are highlighted in Table 3 to deeply understand the impact of each optimisation scenario on the cooling performance of the proposed green roof.

The results from the best case scenarios for each optimisation parameter were compared through Tukey's honestly significant difference (HSD) test [83] and ANOVA test using the F-statistics [84] approach to thoroughly understand the statistical dependence of the different optimised parameters with respect to the effect they have on air temperature reduction. Tukey's HSD test was performed to determine the impact each optimised parameter had on the maximum reduction in air temperature at rooftop level. The best-case scenarios for all the optimisation parameters, such as LAI, plant height, soil moisture and added tree cover, were analysed to determine the statical dependence of the parameters.

Fig. 23 shows the comparison of the mean differences among the best-performing test cases in each optimisation scenario extracted from the Tukey HSD analysis. When the best-case scenario of LAI (2.5 m^2/m^2) was compared with the best-case scenario of plant height (0.6 m), the mean difference was −0.5129, with a p-value of 0.3593. When the best-case scenario of LAI (2.5 m^2/m^2) was compared with the best-case scenario of soil moisture (0.6), a mean difference of −0.3223 was observed, with a p-value of 0.6984. Likewise, the comparison of the best-case scenario of LAI (2.5 m^2/m^2) with the best-case scenario of tree

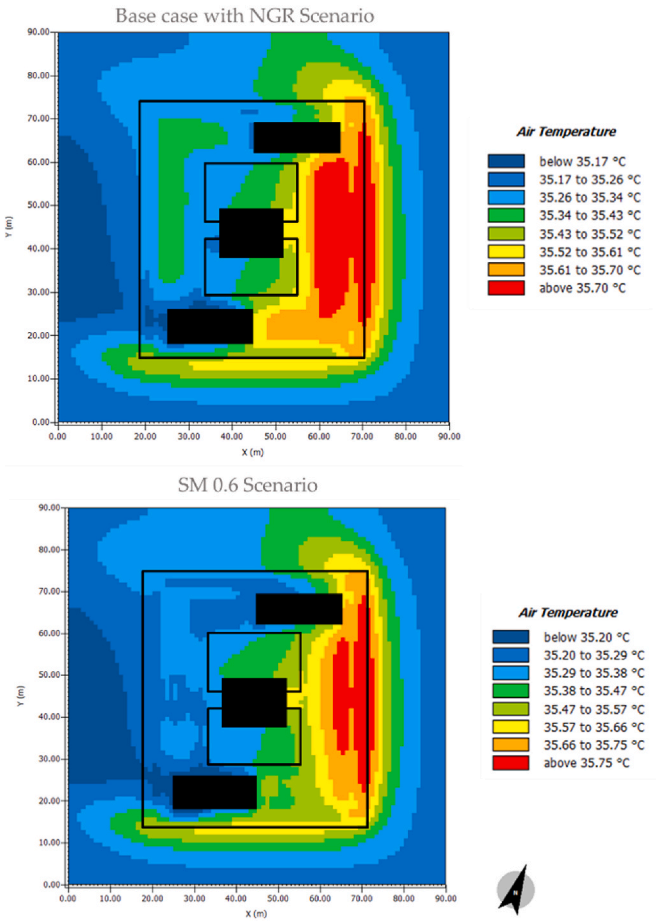

Fig. 19. Air temperature spatial distribution variations in the base case scenario with no green roof (top) and optimisation scenario 3 (soil moisture = 0.6; bottom) captured at 1.5 m from the roof. (For interpretation of the references to colour in this figure legend, the reader is referred to the Web version of this article.)

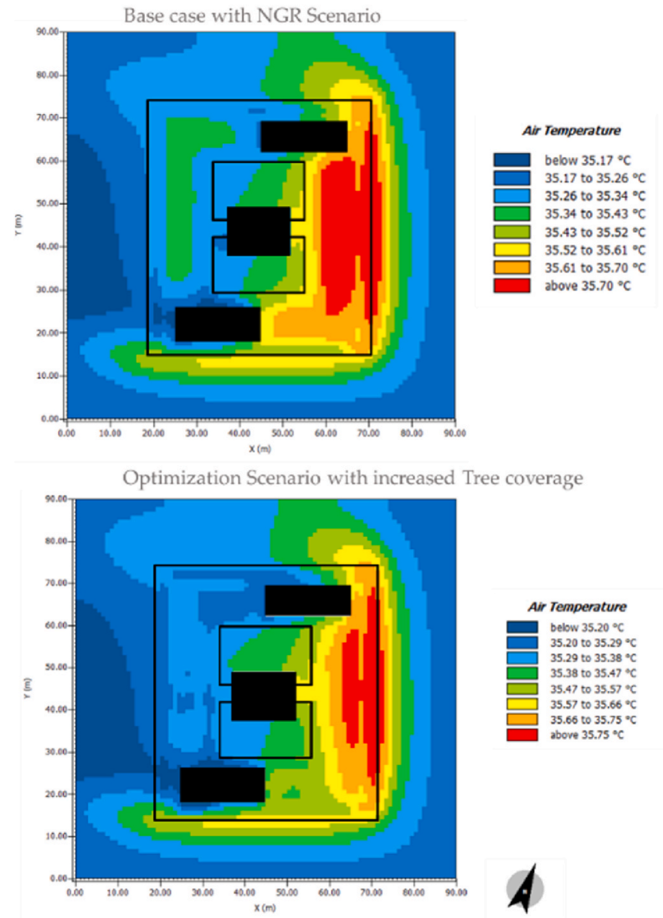

Fig. 21. Air temperature spatial distributions in the base case scenario with no green roof (top) and optimisation scenario 4 (bottom) captured at 1.5 m from the roof. (For interpretation of the references to colour in this figure legend, the reader is referred to the Web version of this article.)

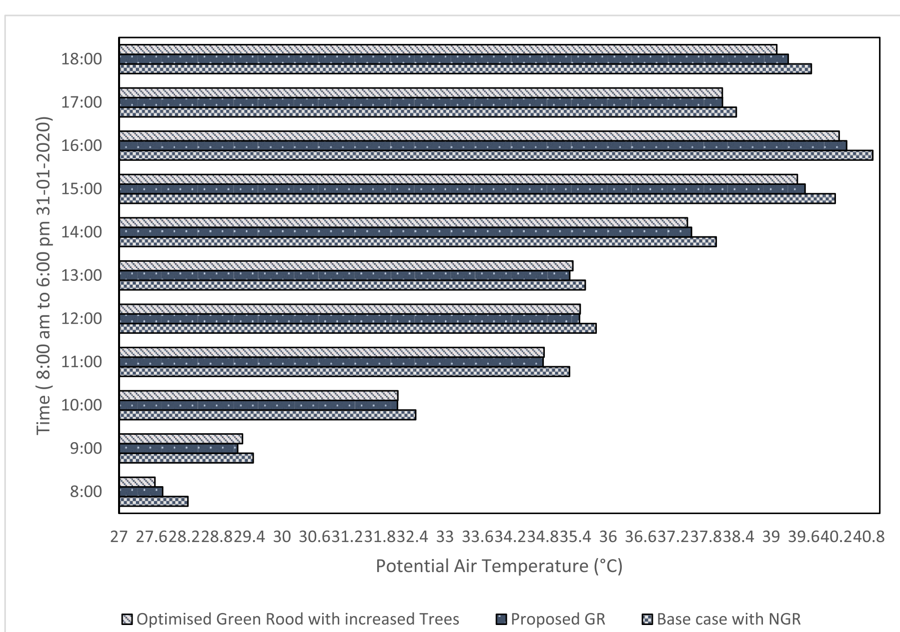

Fig. 20. Comparison of air temperature values in the base case scenario with no green roof, proposed green roof scenario and optimisation scenario 4 on 31 January 2020 captured at 1.5 m from the roof. (For interpretation of the references to colour in this figure legend, the reader is referred to the Web version of this article.)

Table 3
Optimum values for each optimisation scenario (highlighted) and the associated cooling impact.

	Proposed Green Roof – Base Case Scenario			
Optimisation Scenario 1– Proposed Green Roof	LAI (m^2 / m^2)	0.69 (average LAI of the proposed green roof)	0.71	1
		1.08	1.50	
		2.5	1.55	
Scenario 2– Proposed Green Roof	Plant height (m)	0.2	0.355	3
		0.4	0.53	
		0.33 (average plant height of the proposed green roof)	0.71	
		0.6	0.74	
Scenario 3– Proposed Green Roof	Increased soil moisture [0.1]	0.1	0.355	2
		0.3	0.5325	
		0.5 (default soil Moisture in the proposed green roof)	0.71	
		0.6	1.50	
Scenario 4– Proposed Green Roof	Replacement with tree coverage (%)	+ 50 %	1.50	2

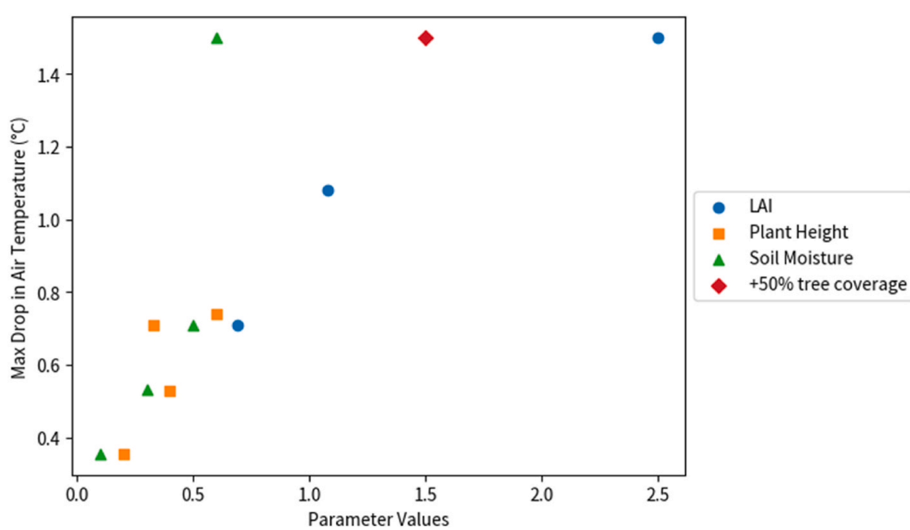

Fig. 22. Maximum drop in air temperature across parameter values in the different optimisation scenarios.

coverage (+50%) demonstrated a mean difference of 0.4033, with a p-value of 0.7993. When the best-case scenario of plant height (0.6 m) was compared with the best-case scenario of soil moisture (0.6), the mean difference was 0.1906, and the p-value was 0.8927. Additionally, when the best-case scenario for plant height (0.6 m) was compared with the best-case scenario for tree coverage, a mean difference of 0.9162 and a p-value of 0.2197 were obtained. The comparison of the best-case scenario for soil moisture (0.6) with the best-case scenario for added tree coverage yielded a mean difference of 0.7256 and a p-value of 0.3854.

Fig. 22 shows that the optimum thermal performance of the proposed green roof was observed when LAI was set to 2.5 (m^2/m^2; air temperature reduction of 1.55 °C), soil moisture was set to 0.6 (air temperature reduction of 1.5 °C) and 50% tree coverage was added to the proposed green roof (air temperature reduction of 1.5 °C).

Tukey's HSD analysis revealed that the statistical differences across each optimised parameter were equally distributed across all the best-case optimisation scenarios of LAI (2.5 m^2/m^2), soil moisture (0.6), plant height (0.6 m) and added tree cover (50%), as indicated in Fig. 23. The ANOVA test was used to compare the variations among the groups (different parameters) and within groups (with each parameter value).

The ANOVA test showed a p-value of 0.1824 and an F-statistic value of 2.0718 in all the optimisation scenarios. The variability between the groups was not significantly higher than the variability within the groups. The uniformity of the F-statistic across the different optimisation scenarios showed that each scenario had an equal impact on the observed results on air temperature reduction, and no scenario differed significantly from the others.

Fig. 24 shows the air temperature variation for the optimum values in each optimisation scenario and its comparison with the base case and proposed green roof scenarios. According to Fig. 24, the maximum

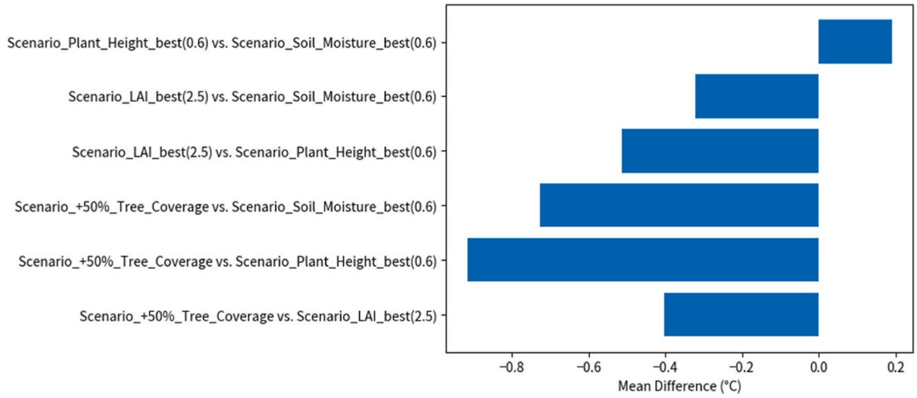

Fig. 23. Comparison of Tukey's HSD mean difference values indicating an equal impact across different optimisation scenarios.

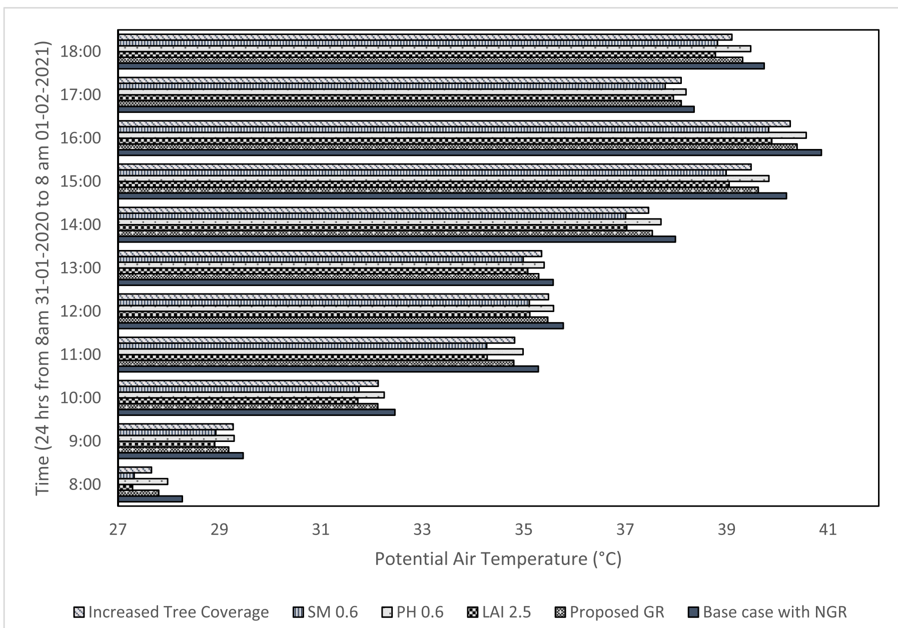

Fig. 24. Comparison of air temperature values between the base case scenario with no green roof and the proposed green roof scenario and the optimum values for each optimisation scenario on 31 January 2020 captured at 1.5 m from the roof. (For interpretation of the references to colour in this figure legend, the reader is referred to the Web version of this article.)

cooling effect was achieved by optimisation scenario 1 when the mean LAI was set to 2.5. In this scenario, a 0.835 °C drop in the mean air temperature was observed compared with the proposed green roof scenario, representing a percentage decrease of approximately 69% relative to the base case. Furthermore, the maximum cooling impact reached 1.55 °C. In optimisation scenario 2 with plant height set at 0.6, the mean air temperature was reduced by 0.74 °C across the rooftop, indicating a percentage decrease of about 53.23%.

In optimisation scenario 3, when the soil moisture was set to 0.6, the optimum result was achieved, and the air temperature was reduced by 1.5 °C, signifying a percentage decrease of approximately 69%. In optimisation scenario 4, when 50% of the proposed green roof was replaced by tree coverage, the air temperature was reduced by 1.5 °C.

The correlation analysis highlighted the strong positive relationships of the parameters, such as LAI, plant height, soil moisture and tree coverage, with the maximum temperature drop, reinforcing their pivotal roles in maximising the cooling impact. This finding is partially in line with that of Zeng's study, which investigated the optimum design settings for green roofs across China and concluded that LAI is the key parameter that affects the thermal performance of green roofs [57]. A similar finding was obtained by a study in South Australia, which reported that LAI is one of the main governing factors that influence the thermal performance of green roofs [58]. This study also demonstrated the insignificant effects of stomata resistance and water availability of the substrate on thermal performance.

Fig. 25 shows the air temperature spatial distributions across the different optimisation scenarios with optimum values for LAI, plant height, soil moisture and tree coverage at the rooftop level. A significant reduction in air temperature was obtained as a result of the proposed green roof, and additional reductions in air temperature brought about by the optimum design settings were observed.

6. Effects on human thermal comfort

Various thermal indices, such as PET, UTCI and Outdoor Standard Effective Temperature (OUT_SET*), were calibrated to assess local thermal comfort conditions. Among these indices, PET is the most commonly used according to previous reviews [85–88]. PET uses the ambient temperature in a standard indoor environment, devoid of wind and direct sunlight, where the body's heat exchange matches that which

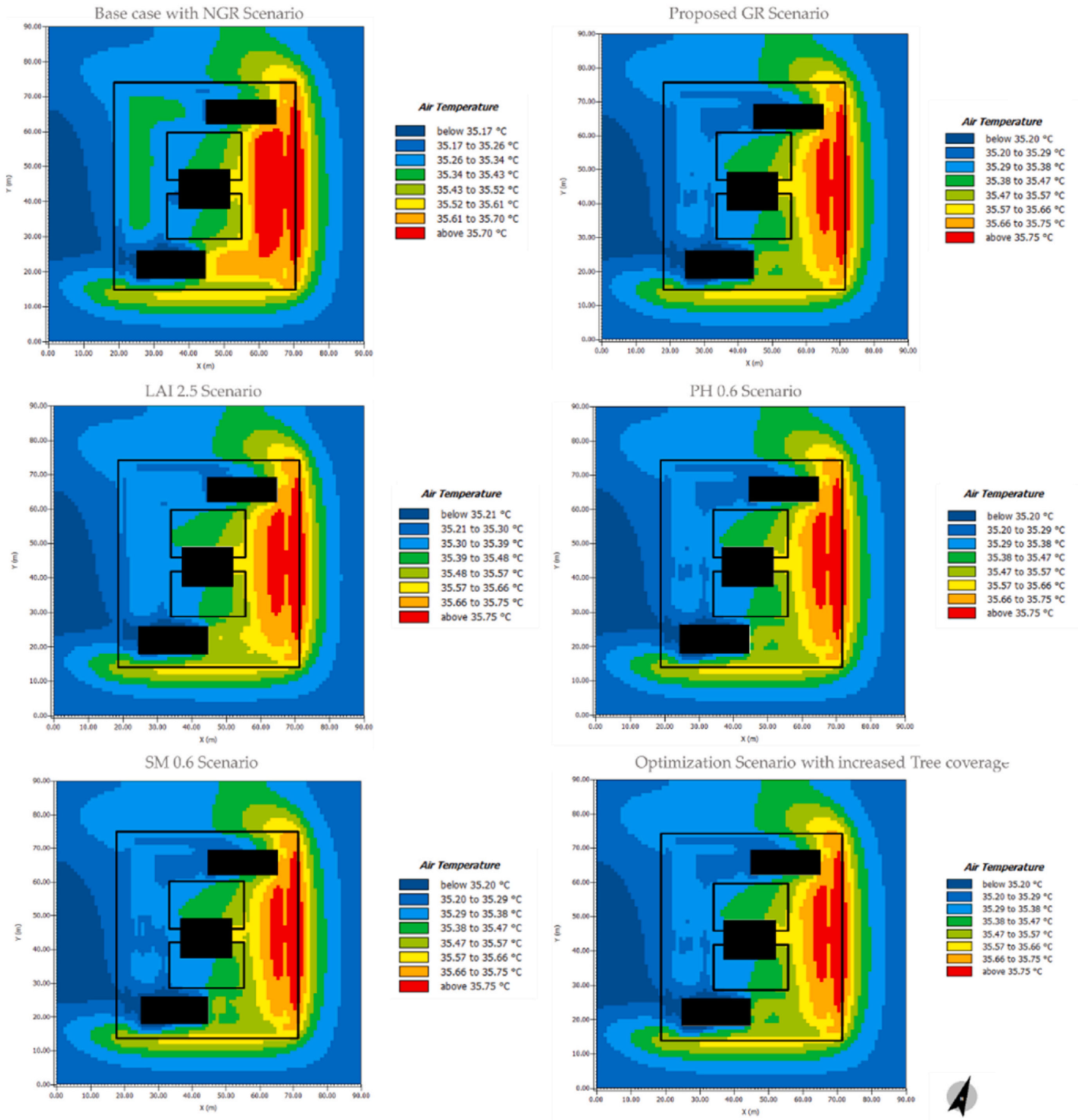

Fig. 25. Air temperature spatial distributions in the base case scenario with no green roof (top left), proposed green roof scenario (top right) and optimisation scenarios with the optimum value for each parameter captured at a height of 1.5 m from the roof (middle and bottom). (For interpretation of the references to colour in this figure legend, the reader is referred to the Web version of this article.)

occurs in intricate outdoor settings being evaluated. This metric allows individuals without specialised knowledge to gauge the cumulative impacts of multifaceted outdoor thermal circumstances in relation to their own indoor experiences. Table 4 presents the spectrum of PET values. The PET index, which is regarded as a biometeorological factor [89,90], delineates personal thermal perception by considering the equilibrium of human body heat and is presented in degrees Celsius. Notably, this parameter is more comprehensible than other metrics, such as the predicted mean vote percentage.

In this study, the effects of the proposed green roof and each optimisation scenario on human thermal comfort were quantified using PET and a postprocessing tool integrated in ENVI-met called 'Biomet' [91]. Biomet incorporates all meteorological data from simulation outputs and personal parameters (e.g. age, gender, height, weight, clothing value and metabolism rate) that can be adjusted by the user. In this study, PET was calculated based on a 35-year-old man with 1.75 m height, 75 kg weight, 164.49 W/m^2 metabolic rate and 0.9 m^{2}K/W clothing insulation.

Table 4
PET values and grade of physiological stress.

PET (°C)	Thermal perception	Physiological stress grade
<4 °C	Very cold	Extreme cold stress
4 °C–8 °C	Cold	Strong cold stress
8 °C–13 °C	Cool	Moderate cold stress
13 °C–18 °C	Slightly cool	Slight cold stress
18 °C–23 °C	Comfortable	No thermal stress
23 °C–29 °C	Slightly warm	Slight heat stress
29 °C–35 °C	Warm	Moderate heat stress
35 °C–41 °C	Hot	Strong heat stress
>41	Very hot	Extreme heat stress

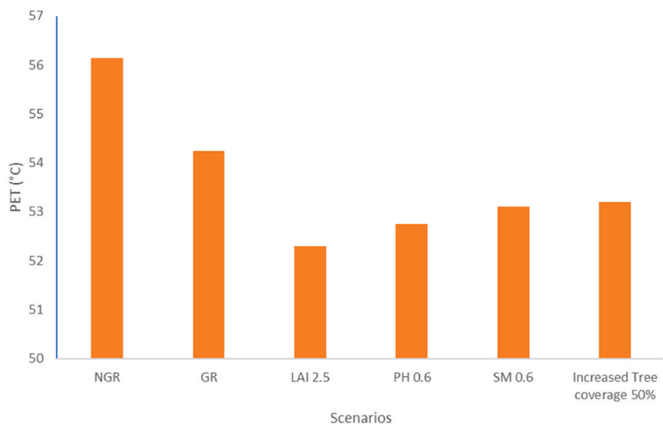

Fig. 26. PET variations in the base case scenario with no green roof, proposed green roof scenario and optimisation scenarios with optimum values for each parameter on 31 January 2020 captured at 1.5 m from the roof. (For interpretation of the references to colour in this figure legend, the reader is referred to the Web version of this article.)

Fig. 26 shows the variations in PET in the existing scenario with no green roof, proposed green roof scenario and optimisation scenarios with optimum settings. The variations in PET were monitored at the rooftop level from 6 a.m. to 6 pm.

The comparison of the PET levels in the base case scenario with no green roof and in the proposed green roof scenario showed that the proposed green roof could be conveniently implemented with respect to users' comfort because of the improvements in the PET level. The average magnitude of PET was reduced by 1.44 °C by the green roof implementation at the rooftop level (21.5 m from the rooftop). This result is in line with the findings of [92], where the thermal effects of installing an intensive green roof were quantified using the ENVI-met model. The study showed that on a hot summer day, green roofs can improve thermal comfort at the roof level.

The maximum PET reduction was obtained at noon time, with 2.382 °C improvement at 12 p.m., and the minimum reduction was observed in the early evening, with a 0.601 °C decrease in the mean PET value at 5 p.m. These findings confirm the results of Adhikari and Savvas, who showed that outdoor thermal comfort at the rooftop level is considerably decreased by green roof installation (~1 °C-1.5 °C) [93].

Fig. 26 indicates that optimisation scenario 1 with LAI of 2.5 resulted in the highest level of improvement in users' thermal comfort, with a reduction of 2.382 °C (6.76% reduction) in PET. This improvement was attributed to the role played by vegetation in reducing the air and surface temperatures through shading and evapotranspiration. The results also showed a direct correlation between the increase in vegetation LAI and improvements in thermal comfort.

The second most successful optimisation scenario for thermal comfort improvement was optimisation scenario 2, which involved increasing the mean plant height to 0.6 m, increasing soil moisture to 0.6, and adding tree coverage. However, the improvements in PET resulting from these modifications were less significant compared with those from the LAI and plant height optimised values. Nevertheless, these combined modifications resulted in a reduction of 1.25 °C (3.47% reduction) in PET compared with the base case scenario with no green roof.

Although all the scenarios shown in Fig. 26 belong to the 'very hot' classification, past studies have shown that even a small reduction in the PET level contributes to the health and well-being of urban dwellers [94, 95]. None of the proposed scenarios produced significant thermal comfort improvements at the pedestrian level. Chen reported similar findings on the cooling impact of green roofs on pedestrians in high-rise buildings; the effect is minimal due to the height of the roofs [49]. Likewise, a study on a green roof situated at a height of 6 m (equivalent to a two-story building) showed that thermal comfort at the street level was not enhanced [96].

Fig. 27 presents the spatial distributions of PET for the base case and proposed green roof scenarios at 1.5 m above the rooftop and from the ground level. The proposed green roof scenario contributed to the improvement of thermal comfort considerably due to the lower surface temperature of the vegetation as opposed to the high values for the paved areas in the existing scenario with no green roof. The increased coverage of the blue zones and the reduction in the red zones near the

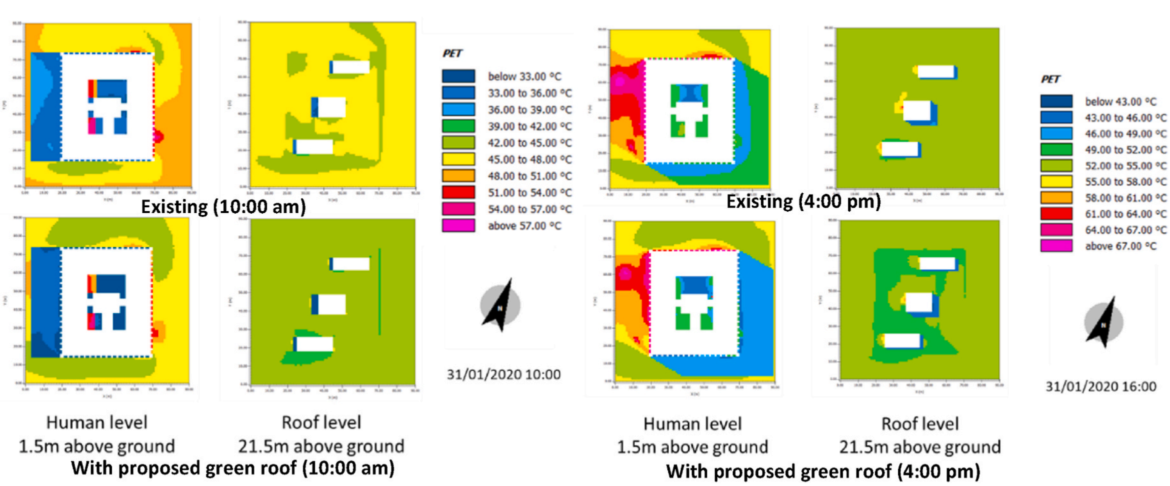

Fig. 27. Spatial distributions of PET in the base case scenario with no green roof and proposed green roof scenario captured at pedestrian and rooftop levels at 10 a.m. (left) and 4 p.m. (right) on 31 January 2020. (For interpretation of the references to colour in this figure legend, the reader is referred to the Web version of this article.)

buildings proved the effectiveness of the proposed green roof and optimisation scenarios in improving pedestrian thermal comfort at the rooftop level. These findings are in line with the results of previous studies that showed that green roofs contribute to improved thermal comfort at the rooftop level [97].

7. Conclusion

Metropolitan or urban centres, which are anticipated to experience substantial temperature rises due to forthcoming climate changes, can derive considerable advantages from implementing green roofs. These benefits, however, are manifested within a limited vicinity of the installation. Therefore, prudent pre-investment planning for green roofs is essential to optimise health benefits and address UHI effects.

Given the urban consolidation in Melbourne and the frequent heat waves caused by the UHI effect, urban overheating needs to be mitigated to minimise the adverse effects, including heat-related mortality and morbidity, on public health. UHI also adversely affects building energy consumption. The building energy consumption in urban areas is determined not only by envelope and equipment features. UHI and the immediate surrounding can also affect the energy performance of buildings located in densely built areas. Therefore, UHI mitigation can result in considerable energy savings in cooling energy needs in summer.

This study examined the effect of intensive green roof implementation on UHI and thermal comfort at the Treasury Place in Melbourne. The effectiveness of the thermal performance of the proposed green roof was assessed using the microclimatic ENVI-met model. The results showed that the proposed green roof can reduce the roof-level daytime air temperature by 1.5 °C and improve rooftop-level thermal comfort by 2.38 °C on a hot summer day. The maximum cooling impact values were produced by optimisation scenario 1 (increased LAI to 2.5), optimisation scenario 2 (increased plant height to 0.3), optimisation scenario 3 (increased soil moisture to 0.6) and optimisation scenario 4 (adding 50% tree coverage). The statistical analysis revealed that all the optimisation scenarios had an equal cooling effect. The parameters LAI, plant height, soil moisture and tree coverage (combined) should be optimised to achieve the best cooling effect.

According to the results, the green roof had a negligible effect on street-level air temperature and PET. The height of the building restricted the green roof's cooling performance to the podium level. These findings indicate that rooftop greening is not an effective mitigation measure for UHI and heat stress at the street level. However, optimised green roofs contribute to improved thermal comfort and UHI mitigation at the rooftop level.

This study confirmed that green roof retrofits offer a strategy for reducing the UHI effect at the Treasury Place in Melbourne. The implementation of green roofs for other buildings in the CBD of Melbourne will exert a remarkable cooling effect on the urban microclimate and provide a viable solution for large-scale UHI mitigation. This study concludes that when selecting the green roof, the key variables that play major roles in the roof's cooling potential (e.g. LAI, soil moisture, plant height and vegetation type) must be considered. According to this study, priority should be given to LAI when aiming for enhanced thermal performance of green roofs in temperate climates. This study suggests that the installation of green roofs should be emphasised in future effect-oriented and sustainable urban planning assessments, especially for inner-city commercial buildings with certain operation hours.

CRediT authorship contribution statement

E. Jamei: Writing – original draft, Validation, Supervision, Methodology, Formal analysis, Conceptualization. **G. Thirunavukkarasu:** Writing – original draft, Visualization, Validation, Methodology, Formal analysis, Conceptualization. **H.W. Chau:** Writing – review & editing, Software, Investigation. **M. Seyedmahmoudian:** Writing – review & editing, Supervision, Software, Investigation. **A. Stojcevski:** Writing – review & editing, Supervision, Investigation. **Saad Mekhilef:** Writing – review & editing, Project administration, Methodology, Formal analysis.

Declaration of competing interest

We also declare no conflict of interest in this project.

Data availability

The authors do not have permission to share data.

Acknowledgement

We would like to thank the City of Melbourne and the Department of Environment, Land, Water and Planning for funding our project titled "Quantifying and optimizing the impact of green roof coverage on UHI, and outdoor thermal comfort" through the 'Green Our Rooftop' grant (GOR0052019).

References

[1] K.C. Seto, B. Güneralp, L.R. Hutyra, Global forecasts of urban expansion to 2030 and direct impacts on biodiversity and carbon pools, Proc. Natl. Acad. Sci. USA 109 (40) (2012) 16083–16088.
[2] S. Kato, Y. Yamaguchi, Estimation of storage heat flux in an urban area using ASTER data, Rem. Sens. Environ. 110 (1) (2007) 1–17.
[3] E. Di Giuseppe, M. D'orazio, Assessment of the effectiveness of cool and green roofs for the mitigation of the Heat Island effect and for the improvement of thermal comfort in Nearly Zero Energy Building, Architect. Sci. Rev. 58 (2) (2015) 134–143.
[4] M. Santamouris, A. Synnefa, T. Karlessi, Using advanced cool materials in the urban built environment to mitigate heat islands and improve thermal comfort conditions, Sol. Energy 85 (12) (2011) 3085–3102.
[5] M. Santamouris, Cooling the cities – a review of reflective and green roof mitigation technologies to fight heat island and improve comfort in urban environments, Sol. Energy 103 (2014) 682–703.
[6] Y. Sun, G. Augenbroe, Urban heat island effect on energy application studies of office buildings, Energy Build. 77 (2014) 171–179.
[7] M. Santamouris, Energy and Climate in the Urban Built Environment, Routledge, 2013.
[8] J.G. Carter, Climate change adaptation in European cities, Curr. Opin. Environ. Sustain. 3 (3) (2011) 193–198.
[9] U. Berardi, A. GhaffarianHoseini, A. GhaffarianHoseini, State-of-the-art analysis of the environmental benefits of green roofs, Appl. Energy 115 (2014) 411–428.
[10] Green engineering principles promote low-impact development, Environ. Sci. Technol. 39 (16) (2005) 338A–344A.
[11] M. Abuseif, Z. Gou, A review of roofing methods: construction features, heat reduction, payback period and climatic responsiveness, Energies 11 (11) (2018) 3196.
[12] Y. He, et al., Thermal and energy performance of green roof and cool roof: a comparison study in Shanghai area, J. Clean. Prod. 267 (2020), 122205.
[13] H.M. Imran, et al., Effectiveness of green and cool roofs in mitigating urban heat island effects during a heatwave event in the city of Melbourne in southeast Australia, J. Clean. Prod. 197 (2018) 393–405.
[14] D.J. Sailor, A green roof model for building energy simulation programs, Energy Build. 40 (8) (2008) 1466–1478.
[15] Å. Ode Sang, P. Thorpert, A.-M. Fransson, Planning, designing, and managing green roofs and green walls for public health–an ecosystem services approach, Front. Ecol. Evolution 10 (2022), 804500.
[16] S. Koley, Sustainability appraisal of arsenic mitigation policy innovations in West Bengal, India, Infrastructure Asset Manag 10 (1) (2022) 17–37.
[17] A.M. Hassan, UMC-based models: an integrating UMC performance analysis and numerical methods, Renew. Sustain. Energy Rev. 181 (2023), 113307.
[18] C.-F. Chen, Performance evaluation and development strategies for green roofs in Taiwan: a review, Ecol. Eng. 52 (2013) 51–58.
[19] D. Townshend, A. Duggie, Study on Green Roof Application in Hong Kong, Architectural services department, 2007.
[20] S. Vera, et al., Influence of vegetation, substrate, and thermal insulation of an extensive vegetated roof on the thermal performance of retail stores in semiarid and marine climates, Energy Build. 146 (2017) 312–321.
[21] BCC, *Proposed Citywide Amendment - Rooftop Gardens And Landscaped*, 2020.
[22] J.M. Murphy, D.M. H S, G.J. Jenkins, P.M. Booman, B.B.B. Booth, C.C. Brown, et al., UK Climate Projections Science Report: Climate Change Projections, Met Office Hadley Centre, Exeter, 2009.
[23] G.A. Meehl, C. Tebaldi, More intense, more frequent, and longer lasting heat waves in the 21st century, Science 305 (5686) (2004) 994–997.
[24] S.E. Gill, et al., Adapting cities for climate change: the role of the green infrastructure, Built. Environ. 33 (1) (2007) 115–133.
[25] D.E. Bowler, et al., Urban greening to cool towns and cities: a systematic review of the empirical evidence, Landsc. Urban Plann. 97 (3) (2010) 147–155.

[26] R.W. Cameron, et al., The domestic garden–Its contribution to urban green infrastructure, Urban For. Urban Green. 11 (2) (2012) 129–137.
[27] R.W. Cameron, T. Blanuša, Green infrastructure and ecosystem services–is the devil in the detail? Ann. Bot. 118 (3) (2016) 377–391.
[28] L.L. Peng, C.Y. Jim, Green-roof effects on neighborhood microclimate and human thermal sensation, Energies 6 (2) (2013) 598–618.
[29] L.M. Cavanaugh, Redefining the green roof, J. Architect. Eng. 14 (1) (2008) 4–6.
[30] K.L. Getter, D.B. Rowe, The role of extensive green roofs in sustainable development, Hortscience 41 (5) (2006) 1276–1285.
[31] J.C. Berndtsson, Green roof performance towards management of runoff water quantity and quality: a review, Ecol. Eng. 36 (4) (2010) 351–360.
[32] E. Fassman, R. Simcock, Moisture measurements as performance criteria for extensive living roof substrates, J. Environ. Eng. 138 (8) (2012) 841–851.
[33] D. Roehr, E. Fassman-Beck, Living Roofs in Integrated Urban Water Systems, Routledge, 2015.
[34] Y. Ashie, Management of urban heat environment, in: Urban Environmental Management and Technology, Springer, 2008, pp. 215–238.
[35] F. Butera, Towards the renewable built environment, in: Urban Energy Transition, Elsevier, 2008, pp. 327–364.
[36] T. Dahl, et al., Climate and Architecture, Routledge, 2010.
[37] E. Erell, D. Pearlmutter, T. Williamson, Urban Microclimate: Designing the Spaces between Buildings, Routledge, 2012.
[38] L.M. Gartland, Heat Islands: Understanding and Mitigating Heat in Urban Areas, Routledge, 2012.
[39] T.R. Oke, Towards better scientific communication in urban climate, Theor. Appl. Climatol. 84 (2006) 179–190.
[40] S. Huttner, M. Bruse, Numerical modeling of the urban climate–a preview on ENVI-met 4.0, in: 7th International Conference on Urban Climate ICUC-7, Citeseer, Yokohama, Japan, 2009.
[41] C. Skelhorn, S. Lindley, G. Levermore, The impact of vegetation types on air and surface temperatures in a temperate city: a fine scale assessment in Manchester, UK, Landsc. Urban Plann. 121 (2014) 129–140.
[42] ZinCo, Solar Energy and Green Roofs. Retrieved on April 22, 2019 from https://zincogreenroof.com/sites/default/files/2018-07/ ZinCo_Green_Roof_Solar_Energy.pdf. 2018.
[43] B. Bass, et al., The Impact of Green Roofs on Toronto's Urban Heat Island, 2003.
[44] M. Santamouris, Cooling the cities–a review of reflective and green roof mitigation technologies to fight heat island and improve comfort in urban environments, Sol. Energy 103 (2014) 682–703.
[45] I.D. Stewart, T.R. Oke, Local climate zones for urban temperature studies, Bull. Am. Meteorol. Soc. 93 (12) (2012) 1879–1900.
[46] K.R. Smith, P.J. Roebber, Green roof mitigation potential for a proxy future climate scenario in Chicago, Illinois, J. Appl. Meteorol. Climatol. 50 (3) (2011) 507–522.
[47] C. Rosenzweig, W. Solecki, R. Slosberg, Mitigating New York City's Heat Island with Urban Forestry, Living Roofs, and Light Surfaces, A report to the New York State Energy Research and Development Authority, 2006.
[48] E. Ng, et al., A study on the cooling effects of greening in a high-density city: an experience from Hong Kong, Build. Environ. 47 (2012) 256–271.
[49] H. Chen, et al., Study on mitigation measures for outdoor thermal environment on present urban blocks in Tokyo using coupled simulation, Build. Environ. 44 (11) (2009) 2290–2299.
[50] R.M. Lazzarin, F. Castellotti, F. Busato, Experimental measurements and numerical modelling of a green roof, Energy Build. 37 (12) (2005) 1260–1267.
[51] P. Bevilacqua, R. Bruno, N. Arcuri, Green roofs in a Mediterranean climate: energy performances based on in-situ experimental data, Renew. Energy 152 (2020) 1414–1430.
[52] M. Köhler, M. Schmidt, M. Laar, Green roofs as a contribution to reduce urban heat islands, in: Proceedings of the World Climate and Energy Event, Rio de Janeiro, Brazil, 2003, pp. 1–5.
[53] F. Balany, et al., Studying the effect of blue-green infrastructure on microclimate and human thermal comfort in melbourne's central business district, Sustainability 14 (15) (2022) 9057.
[54] H.M. Imran, et al., Effectiveness of green and cool roofs in mitigating urban heat island effects during a heatwave event in the city of Melbourne in southeast Australia, J. Clean. Prod. 197 (2018) 393–405.
[55] S.S. Herrera-Gomez, A. Quevedo-Nolasco, L. Pérez-Urrestarazu, The role of green roofs in climate change mitigation. A case study in Seville (Spain), Build. Environ. 123 (2017) 575–584.
[56] C.Y. Jim, S. Tsang, Biophysical properties and thermal performance of an intensive green roof, Build. Environ. 46 (6) (2011) 1263–1274.
[57] C. Zeng, et al., Optimal parameters of green roofs in representative cities of four climate zones in China: a simulation study, Energy Build. 150 (2017) 118–131.
[58] A. Pianella, et al., Substrate depth, vegetation and irrigation affect green roof thermal performance in a mediterranean type climate, Sustainability 9 (8) (2017) 1451.
[59] T. Almaaitah, et al., The potential of Blue-Green infrastructure as a climate change adaptation strategy: a systematic literature review, Blue-Green Systems 3 (1) (2021) 223–248.
[60] C. Feng, Q. Meng, Y. Zhang, Theoretical and experimental analysis of the energy balance of extensive green roofs, Energy Build. 42 (6) (2010) 959–965.
[61] G. Kokogiannakis, J. Darkwa, Support for the integration of green roof constructions within Chinese building energy performance policies, Energy 65 (2014) 71–79.
[62] C.Y. Jim, Passive warming of indoor space induced by tropical green roof in winter, Energy 68 (2014) 272–282.
[63] A. Pianella, et al., Effects of Design and Operating Parameters on Green Roof Thermal Performance in Melbourne, 2016.
[64] A. Pianella, et al., Effects of substrate depth and native plants on green roof thermal performance in South-East Australia, in: IOP Conference Series: Earth and Environmental Science, IOP Publishing, 2020.
[65] A. Pianella, The Thermal Performance of Green Roofs in Hot and Dry Mediterranean Type Climate, 2018.
[66] M.C. Peel, B.L. Finlayson, T.A. McMahon, Updated world map of the Köppen-Geiger climate classification, Hydrol. Earth Syst. Sci. 11 (5) (2007) 1633–1644.
[67] A. Bom, Northern Territory in December 2019: Hottest December on Record and Very Dry, 2019 [cited 2021; Available from: http://www.bom.gov.au/climate/current/month/nt/archive/201912.summary.shtml.
[68] Bom, A. Wind speed and direction in the Melbourne Olympic Park *(Station number: 086282) at 15:00 during summertime* 2020 [cited 2021 13/06/2021]; Available from: http://www.bom.gov.au/cgi-bin/climate/cgi_bin_scripts/windrose_selector.cgi?period=Summer&type=3&location=86282&Submit=Get+Rose.
[69] M. Bruse, ENVI-Met 3.0: Updated Model Overview, University of Bochum, 2004. Retrieved from: www.envi-met.com.
[70] G. Lobaccaro, J.A. Acero, Comparative analysis of green actions to improve outdoor thermal comfort inside typical urban street canyons, Urban Clim. 14 (2015) 251–267.
[71] H. Simon, et al., Modeling transpiration and leaf temperature of urban trees–a case study evaluating the microclimate model ENVI-met against measurement data, Landsc. Urban Plann. 174 (2018) 33–40.
[72] A. Forouzandeh, Numerical modeling validation for the microclimate thermal condition of semi-closed courtyard spaces between buildings, Sustain. Cities Soc. 36 (2018) 327–345.
[73] H. Lee, H. Mayer, L. Chen, Contribution of trees and grasslands to the mitigation of human heat stress in a residential district of Freiburg, Southwest Germany, Landsc. Urban Plann. 148 (2016) 37–50.
[74] P. Höppe, The physiological equivalent temperature–a universal index for the biometeorological assessment of the thermal environment, Int. J. Biometeorol. 43 (1999) 71–75.
[75] A. Matzarakis, H. Mayer, M.G. Iziomon, Applications of a universal thermal index: physiological equivalent temperature, Int. J. Biometeorol. 43 (1999) 76–84.
[76] V. Vdi, *Part I: Environmental Meteorology, Methods For the Human Biometeorological Evaluation Of Climate And Air Quality For the Urban And Regional Planning At Regional Level. Part I: Climate.* Part I: Climate, 3787, Beuth, Berlin, 1998.
[77] F. Ali-Toudert, H. Mayer, Numerical study on the effects of aspect ratio and orientation of an urban street canyon on outdoor thermal comfort in hot and dry climate, Build. Environ. 41 (2) (2006) 94–108.
[78] M. Fahmy, S. Sharples, M. Yahiya, LAI based trees selection for mid latitude urban developments: a microclimatic study in Cairo, Egypt, Build. Environ. 45 (2) (2010) 345–357.
[79] S. Wilkinson, et al., Evaluating the thermal performance of retrofitted lightweight green roofs and walls in Sydney and Rio de Janeiro, Procedia Eng. 180 (2017) 231–240.
[80] A. Cortes, et al., Evaluating mitigation strategies for urban heat island in Mandaue City using ENVI-met, J. Urban Manag. 11 (1) (2022) 97–106.
[81] M. Lin, et al., Modeling green roofs' cooling effect in high-density urban areas based on law of diminishing marginal utility of the cooling efficiency: a case study of Xiamen Island, China, J. Clean. Prod. 316 (2021), 128277.
[82] X. Zheng, et al., Green roof cooling and carbon mitigation benefits in a subtropical city, Urban For. Urban Green. 86 (2023), 128018.
[83] H. Abdi, L.J. Williams, Tukey's honestly significant difference (HSD) test, Encyclopedia Res. design 3 (1) (2010) 1–5.
[84] L. St, S. Wold, Analysis of variance (ANOVA), Chemometr. Intell. Lab. Syst. 6 (4) (1989) 259–272.
[85] J. Li, N. Liu, The perception, optimization strategies and prospects of outdoor thermal comfort in China: a review, Build. Environ. 170 (2020), 106614.
[86] O. Potchter, et al., Outdoor human thermal perception in various climates: a comprehensive review of approaches, methods and quantification, Sci. Total Environ. 631 (2018) 390–406.
[87] D. Lai, et al., A comprehensive review of thermal comfort studies in urban open spaces, Sci. Total Environ. 742 (2020), 140092.
[88] M. Nikolopoulou, S. Lykoudis, Thermal comfort in outdoor urban spaces: analysis across different European countries, Build. Environ. 41 (11) (2006) 1455–1470.
[89] S.N. Gosling, et al., A glossary for biometeorology, Int. J. Biometeorol. 58 (2014) 277–308.
[90] R.F. Rupp, N.G. Vásquez, R. Lamberts, A review of human thermal comfort in the built environment, Energy Build. 105 (2015) 178–205.
[91] J. Fischereit, K.H. Schlünzen, Evaluation of thermal indices for their applicability in obstacle-resolving meteorology models, Int. J. Biometeorol. 62 (10) (2018) 1887–1900.
[92] M. Knaus, D. Haase, Green roof effects on daytime heat in a prefabricated residential neighbourhood in Berlin, Germany, Urban For. Urban Green. 53 (2020), 126738.
[93] A. Adhikari, W. Savvas, Green roofs for energy efficiency-a simulation study in Australian climates, Environ. Design Guide (88) (2016) 1–23.
[94] A.M. Coutts, et al., Watering our cities: the capacity for Water Sensitive Urban Design to support urban cooling and improve human thermal comfort in the Australian context, Prog. Phys. Geogr. 37 (1) (2013) 2–28.

[95] N. Tapper, et al., Urban populations' vulnerability to climate extremes: mitigating urban heat through technology and water-sensitive urban design, in: Low Carbon Cities, Routledge, 2014, pp. 399–412.
[96] M. Taleghani, D. Sailor, G.A. Ban-Weiss, Micrometeorological simulations to predict the impacts of heat mitigation strategies on pedestrian thermal comfort in a Los Angeles neighborhood, Environ. Res. Lett. 11 (2) (2016), 024003.
[97] D.-i. Jeong, K.-h. Park, B.-g. Song, A comparison between in-situ PET and ENVI-met PET for evaluating outdoor thermal comfort, KIEAE J. 16 (1) (2016) 11–19.